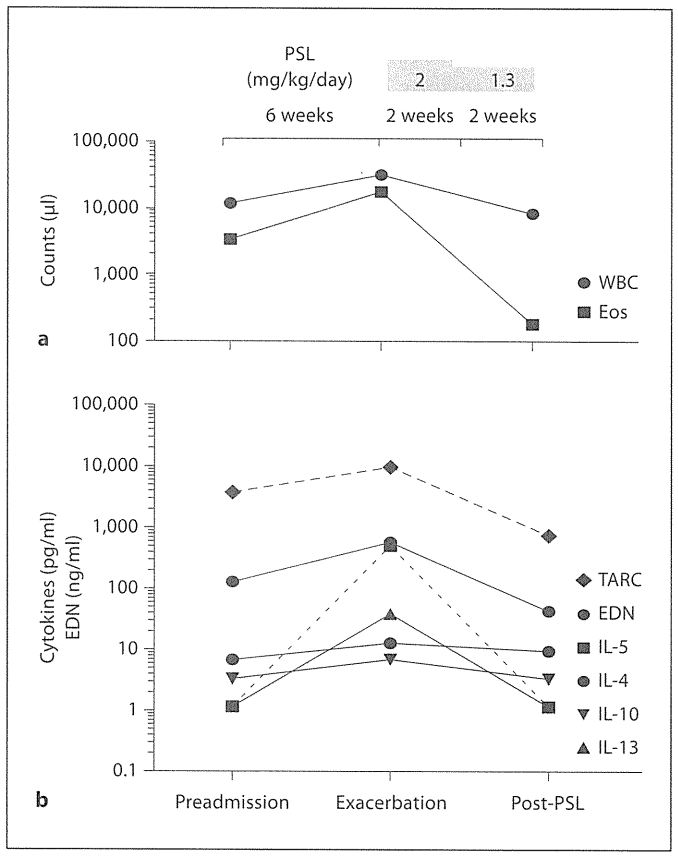

Fig. 3. Course of laboratory data. Peripheral white blood cell, eosinophil, serum cytokine and EDN levels were elevated remarkably at the time of exacerbation. PSL inhibited the white blood cell and eosinophil counts (**a**) and EDN, TARC, IL-5, and IL-13 (**b**). Eos = Eosinophils.

phil-associated pathology [1]. In addition, since the 4th revision of the WHO classification of myeloid neoplasms and acute leukemia, the diagnosis of HES requires exclusion of other acute or chronic myeloid neoplasms, no evidence of phenotypically abnormal and/or clonal T lymphocytes, and absence of both cytogenetic abnormality including rearrangements of *PDGFRA*, *PDGFRB* or *FGFR1* and >2% peripheral blasts or >5% bone marrow blasts [2, 3].

Since HES is extraordinarily rare in children, we first suspected food-induced eosinophilic gastrointestinal disorders or *H. pylori* infection [4–6] as possible causes for the gastrointestinal symptoms and profound eosinophilia. However food elimination and eradication of *H. pylori* did not have any effect. Although lung function was normal, abnormal lung CT findings (fig. 1b, c) suggested significant organ damage associated with eosinophilia. In addition, the bone marrow findings did not show any evidence of secondary eosinophilia. We then diagnosed HES.

HES is predominantly a disease of men (male:female ratio 9:1) and is usually diagnosed between the ages of 20 and 50 years [7]. Katz et al. [8] reported that pediatric HES has a slight male dominance (55.3% male vs. 44.7% female), and the mean age at diagnosis was 8.2 years. The common presenting symptoms in children with HES are fever, arthralgia, and skin rash. Diarrhea and abdominal pain, which were major presenting symptom in this case, are less common in children [8]. Various organs can be involved in HES. Hematologic, cardiovascular, dermatologic, and neurologic manifestations are common [9]. Despite the fact that the patient complained only of gastrointestinal symptoms, radiologic examination strongly suggested that the lungs and bladder were also involved, indicating that systemic screening procedures are necessary in the diagnosis and evaluation of HES.

The lymphocytic variant of HES results from overproduction of eosinophilopoietic cytokines, mainly IL-5, by clonally aberrant T cells. Detection of the aberrant T cell phenotype in peripheral blood by flow cytometry and the presence of T cell receptor clonal rearrangement are required for diagnosis [10, 11]. We could not detect aberrant phenotype T cells by flow cytometry and tried to examine for rearrangements of T cell receptors. However, we could not proceed to the diagnostic step because of poor cooperation of the patient's family. Lymphocytic variant HES are characterized by resistance to imatinib mesylate, normal serum levels of tryptase and vitamin B12, and increasing serum IgE, TARC, and IL-5; our case is consistent with this feature [12].

Regarding the treatment of HES, first-line drugs are oral corticosteroids. Ogbogu et al. [12] reported that 85% of patients experienced a complete or partial response after 1 month of corticosteroid treatment in HES. Parrillo et al. [13] demonstrated an overall corticosteroid response rate of nearly 70% in HES. However, poor therapeutic responses to PSL in children have been reported [8]. Serum TARC levels were reported to be significantly elevated in patients who responded to corticosteroids compared with nonresponders [12]. The present case showed good responses to PSL, and elevated TARC may have been a marker for the therapeutic response to steroids. Hydroxyurea, IFN-α, vincristine, anti-IL-5 antibody, and bone marrow transplantation have been reported to show some efficacy for HES, especially when PSL alone did not control eosinophilia and symptoms [12, 14, 15]. Imatinib mesylate, a tyrosine kinase inhibitor,

given to patients with eosinophilia associated with rearrangements involving PDGFRA produced a response rate of 100% [16, 17]. The overall response rate to imatinib in patients HES without abnormalities of PDGFRA was about 20–40% [12, 18]. Therefore, we administered imatinib mesylate, although the rearrangement of PDGFRA was negative in our case. However, imatinib mesylate did not decrease peripheral eosinophil levels and could not reduce the dose of PSL. Three of 5 (60%) HES patients who received cyclosporine monotherapy achieved a complete or partial response [12]. Cyclosporine could reduce the PSL dose in our patient, so cyclosporine might be effective against HES in spite of only a few reports about cyclosporine against HES.

In summary, we presented a rare case of childhood HES. Despite improvements in medical management, HES remains a serious condition with a poor prognosis for the majority of patients [14]. Moreover, the long-term prognosis in pediatric HES is not well known. Comprehensive diagnostic procedures are vital for the early detection and management of complications in pediatric HES.

Disclosure Statement

The authors declare that no financial or other conflict of interest exists in relation to the contents of this article.

References

1 Chusid MJ, Dale DC, West BC, Wolff SM: The hypereosinophilic syndrome: analysis of fourteen cases with review of the literature. Medicine (Baltimore) 1975;54:1–27.
2 Vardiman JW, Thiele J, Arber DA, Brunning RD, Borowitz MJ, Porwit A, Harris NL, Le Beau MM, Hellstrom-Lindberg E, Tefferi A, Bloomfield CD: The 2008 revision of the World Health Organization (WHO) classification of myeloid neoplasms and acute leukemia: rationale and important changes. Blood 2009;114:937–951.
3 Tefferi A, Vardiman JW: Classification and diagnosis of myeloproliferative neoplasms: The 2008 World Health Organization criteria and point-of-care diagnostic algorithms. Leukemia 2008;22:14–22.
4 Kalantar SJ, Marks R, Lambert JR, Badov D, Talley NJ: Dyspepsia due to eosinophilic gastroenteritis. Dig Dis Sci 1997;42:2327–2332.
5 Muller MJ, Sewell GS: Coexistence of eosinophilic gastroenteritis and helicobacter pylori gastritis: causality versus coincidence. Dig Dis Sci 2001;46:1784–1786.
6 Papadopoulos AA, Tzathas C, Polymeros D, Ladas SD: Symptomatic eosinophilic gastritis cured with *Helicobacter pylori* eradication. Gut 2005;54:1822.
7 Fauci AS, Harley JB, Roberts WC, Ferrans VJ, Gralnick HR, Bjornson BH: NIH conference: the idiopathic hypereosinophilic syndrome. Clinical, pathophysiologic, and therapeutic considerations. Ann Intern Med 1982;97:78–92.
8 Katz HT, Haque SJ, Hsieh FH: Pediatric hypereosinophilic syndrome (HES) differs from adult HES. J Pediatr 2005;146:134–136.
9 Gotlib J, Cools J, Malone JM 3rd, Schrier SL, Gilliland DG, Coutre SE: The FIP1L1-PDGFRalpha fusion tyrosine kinase in hypereosinophilic syndrome and chronic eosinophilic leukemia: Implications for diagnosis, classification, and management. Blood 2004;103:2879–2891.
10 Helbig G, Wieczorkiewicz A, Dziaczkowska-Suszek J, Majewski M, Kyrcz-Krzemien S: T-cell abnormalities are present at high frequencies in patients with hypereosinophilic syndrome. Haematologica 2009;94:1236–1241.
11 Roufosse F, Schandene L, Sibille C, Kennes B, Efira A, Cogan E, Goldman M: T-cell receptor-independent activation of clonal Th2 cells associated with chronic hypereosinophilia. Blood 1999;94:994–1002.
12 Ogbogu PU, Bochner BS, Butterfield JH, Gleich GJ, Huss-Marp J, Kahn JE, Leiferman KM, Nutman TB, Pfab F, Ring J, Rothenberg ME, Roufosse F, Sajous MH, Sheikh J, Simon D, Simon HU, Stein ML, Wardlaw A, Weller PF, Klion AD: Hypereosinophilic syndrome: a multicenter, retrospective analysis of clinical characteristics and response to therapy. J Allergy Clin Immunol 2009;124:1319–1325, e1313.
13 Parrillo JE, Fauci AS, Wolff SM: Therapy of the hypereosinophilic syndrome. Ann Intern Med 1978;89:167–172.
14 Wilkins HJ, Crane MM, Copeland K, Williams WV: Hypereosinophilic syndrome: an update. Am J Hematol 2005;80:148–157.
15 Klion AD, Bochner BS, Gleich GJ, Nutman TB, Rothenberg ME, Simon HU, Wechsler ME, Weller PF, The Hypereosinophilic Syndromes Working Group: Approaches to the treatment of hypereosinophilic syndromes: a workshop summary report. J Allergy Clin Immunol 2006;117:1292–1302.
16 Cools J, DeAngelo DJ, Gotlib J, Stover EH, Legare RD, Cortes J, Kutok J, Clark J, Galinsky I, Griffin JD, Cross NC, Tefferi A, Malone J, Alam R, Schrier SL, Schmid J, Rose M, Vandenberghe P, Verhoef G, Boogaerts M, Wlodarska I, Kantarjian H, Marynen P, Coutre SE, Stone R, Gilliland DG: A tyrosine kinase created by fusion of the PDGFRA and FIP1L1 genes as a therapeutic target of imatinib in idiopathic hypereosinophilic syndrome. N Engl J Med 2003;348:1201–1214.
17 Pardanani A, Reeder T, Porrata LF, Li CY, Tazelaar HD, Baxter EJ, Witzig TE, Cross NC, Tefferi A: Imatinib therapy for hypereosinophilic syndrome and other eosinophilic disorders. Blood 2003;101:3391–3397.
18 Muller AM, Martens UM, Hofmann SC, Bruckner-Tuderman L, Mertelsmann R, Lubbert M: Imatinib mesylate as a novel treatment option for hypereosinophilic syndrome: two case reports and a comprehensive review of the literature. Ann Hematol 2006;85:1–16.

Original Paper

International Archives of Allergy and Immunology

Int Arch Allergy Immunol 2011;155(suppl 1):77–84
DOI: 10.1159/000327434

Published online: June 1, 2011

Differential Effects of Corticosteroids on Serum Eosinophil Cationic Protein and Cytokine Production in Rhinovirus- and Respiratory Syncytial Virus-Induced Acute Exacerbation of Childhood Asthma

Masahiko Kato[a] Yoshiyuki Yamada[a] Kenichi Maruyama[b] Yasuhide Hayashi[c]

Departments of [a]Allergy and Immunology, [b]Internal Medicine and [c]Hematology and Oncology, Gunma Children's Medical Center, Shibukawa, Japan

Key Words

Eosinophil cationic protein · IL-5 · Asthma, childhood · Rhinovirus · Respiratory syncytial virus · Corticosteroids

Abstract

Background: Little information is available on eosinophil activation and the cytokine profile in virus-induced acute exacerbation of bronchial asthma; therefore, we examined the effects of treatments that included systemic corticosteroids on serum eosinophil cationic protein (ECP) and 17 cytokines/chemokines in rhinovirus- and respiratory syncytial (RS) virus-induced acute exacerbation of childhood asthma. ***Methods:*** We measured the peripheral eosinophil count, as well as the serum levels of ECP and 17 types of cytokines/chemokines (IL-1β, 2, 4, 5, 6, 7, 8, 10, 12, 13, and 17 and IFN-γ, TNF-α, GM-CSF, G-CSF, MCP-1, and MIP-1β), using a multiplex bead-based assay in 21 cases of rhinovirus- and 12 cases of RS virus-induced acute exacerbation of childhood asthma and 13 controls. We also compared the clinical data and the effects of systemic corticosteroids on these responses between rhinovirus and RS virus groups. ***Results:*** The serum levels of ECP, IL-5, and IL-6 were significantly elevated in patients with rhinovirus-induced acute exacerbation of asthma compared with controls, while serum IL-1β and IFN-γ were significantly lower in patients with rhinovirus-induced acute exacerbation of asthma than in controls. On the other hand, in RS virus-induced acute exacerbation of asthma, only the peripheral eosinophil count was significantly decreased compared with that in rhinovirus-induced acute exacerbation of asthma and controls. Furthermore, the serum levels of ECP, IL-5, and IL-6 in rhinovirus-induced acute exacerbation of asthma and levels of G-CSF in RS virus-induced acute exacerbation of asthma were significantly reduced after treatments that included systemic corticosteroids, respectively. ***Conclusion:*** These results suggest that the effects of systemic corticosteroids on serum ECP and the cytokine profile are different between rhinovirus- and RS virus-induced acute exacerbation of childhood asthma.

Introduction

Viral infection induces both the development and exacerbations of bronchial asthma [1]. In infants, respiratory syncytial (RS) virus is a leading cause of serious lower respiratory tract infections, including acute bronchi-

KARGER

Fax +41 61 306 12 34
E-Mail karger@karger.ch
www.karger.com

1018–2438/11/1555–0077$38.00/0

Accessible online at:
www.karger.com/iaa

Correspondence to: Dr. Masahiko Kato
Department of Allergy and Immunology, Gunma Children's Medical Center
779 Shimohakoda, Hokkitsu-machi
Shibukawa, Gunma 377-8577 (Japan)
Tel. +81 279 52 3551, E-Mail mkato@gcmc.pref.gunma.jp

olitis. RS virus infection also exacerbates recurrent wheezing attacks in patients with established asthma [2]. A number of case-control studies appear to have established at least a statistical connection between RS virus infection in infancy and the development of recurrent wheezing and asthma in young children [3–8]. In later life, it appears unlikely to be a cause of atopic asthma [3, 5, 8]. On the other hand, rhinovirus infection is a major cause of acute exacerbation of asthma in both adults [9] and children [10]. A recent report showed that the most significant risk factor for the development of preschool childhood wheezing is the occurrence of symptomatic rhinovirus illnesses during infancy [11]. The COAST (Childhood Origins of Asthma) study group also reported that wheezing attacks during childhood (2–16 years of age) can be linked to infection with rhinovirus together with evidence of atopy or eosinophilic airway inflammation [12, 13].

The purpose of this study was to investigate changes in the clinical data and serum levels of eosinophil cationic protein (ECP) and several cytokines and chemokines in rhinovirus- and RS virus-induced acute exacerbation of childhood asthma and to evaluate the effects of corticosteroids treatment on these parameters in 2 groups.

Patients and Methods

Patients

The 62 subjects who were hospitalized with acute respiratory symptoms (acute exacerbation of asthma: 43 males and 19 females; mean/median age 3.5/2.8 years) at Gunma Children's Medical Center between November 1, 2003, and October 31, 2006, were enrolled into this study. All recruited patients had a history of 3 or more separate episodes of recurrent wheezing and documented evidence of wheezing by auscultation. The diagnosis of asthma and its severity in subjects with acute exacerbation of asthma were defined according to the guidelines of the Japanese Society of Pediatric Allergy and Clinical Immunology [14]. The diagnosis of asthma was defined as patients with 3 or more independent episodes of wheezing. The symptom severity score was defined as follows: mild attack = 1, moderate attack = 2, and severe attack = 3. Acute exacerbation of asthma was diagnosed by the emergency department physician based on the presence of wheezing and increased difficulty breathing. Briefly, a mild attack was defined as mild wheezing with stability and no dyspnea and an S_pO_2 of ≥96%; a moderate attack was defined as wheezing with dyspnea, apparent retraction, and an S_pO_2 of 92–95%, and a severe attack was defined as more severe wheezing and dyspnea and an S_pO_2 of ≤91%. Patients with mild and moderate attacks were treated with intravenous infusion, salbutamol and disodium cromoglycate inhalation (3 times/day), and/or intravenous theophylline and prednisolone. Patients who experienced a severe attack were treated with isoproterenol inhalation instead of salbutamol. When the S_pO_2 was ≤95%, oxygen therapy was started. Patients with acute exacerbation of asthma had a history of a cold prior to exacerbation. We excluded children with obvious bacterial infections, congenital heart diseases, and chronic lung diseases, as well as those who showed the presence of a foreign body or had signs of severe infection and those who were immunosuppressed, as these complications could interfere with the assessment of asthma-related outcome measures. The control group included 13 healthy children (8 males and 5 females; mean/median age 3.7/4.2 years) with no symptoms of wheezing at the time of examination. Exclusion criteria for the controls included immunosuppression, the presence of other respiratory tract symptoms, or a history of wheezing and asthma. Goals for matching among asthma and control patients included age and sex. This study was approved by the Ethics Committee of Gunma Children's Medical Center. Informed consent was obtained from parents, and assent was obtained from children when they were old enough (usually over 9 years old).

Virus Detection

Nasal aspirates were obtained from patients during acute exacerbation of asthma. Nasal secretions were aspirated into a mucus trap (attached to wall suction) by inserting the tip of a flexible 5F Argyle suction catheter (Nippon Sherwood, Tokyo, Japan) into the anterior nares. Nasal samples were analyzed for RS virus using antigen detection kits (Becton Dickinson, Franklin Lakes, N.J., USA). The remaining secretions were frozen at −80°C until examination by further reverse transcription polymerase chain reaction (RT-PCR) and then by direct DNA sequencing analysis. The RT-PCR method used for rhinoviruses and RS virus was as previously described [15]. The DNA fragments were purified using a QIAquick PCR Purification kit (QIAGEN), and the nucleotide sequence was determined with an automated DNA sequencer ABI PRISM™ 310 Genetic Analyzer (Applied Biosystems, Foster City, Calif., USA) using a Big Dye Terminator v1.1 cycle sequencing kit (Applied Biosystems) [15]. For identification of the virus, newly determined sequences were compared with those available in the sequences using GenBank DNA databases (http://www.ncbi.nlm.nih.gov) and the standard nucleotide-nucleotide BLAST algorithm. The identities of the sequences were determined on the basis of the highest percentage of total nucleotide match in GenBank.

Serum Eosinophil Cationic Protein and Cytokines/Chemokines

We measured the peripheral eosinophil count and the serum levels of ECP and 17 types of cytokines/chemokines [interleukin (IL)-1β, 2, 4, 5, 6, 7, 8, 10, 12, 13, and 17 and interferon (IFN)-γ, tumor necrosis factor (TNF)-α, granulocyte-macrophage colony-stimulating factor (GM-CSF), granulocyte colony-stimulating factor (G-CSF), monocyte chemoattractant protein (MCP)-1, and macrophage inflammatory protein (MIP)-1β] from 33 acute asthma patients who had not used systemic corticosteroids at the time of examination and from 13 control subjects. We analyzed the effects of the treatments including systemic corticosteroids on these parameters by measuring them both at the time of admission and at the time when wheezing disappeared (mean days after admission 6.8) and then compared each factor before and after treatments in patients with acute exacerbation of asthma. The ECP

Table 1. Characteristics of subjects

	n	Mean/median age (range), years	Male gender %	>1 positive aeroallergen CAP-RAST (positive), %
Rhinovirus-induced acute asthma	21	2.5/2.6 (0.3–5.1)	76.2	68.4
RS virus-induced acute asthma	12	3.4/3.0 (0.8–8.1)	66.7	72.7
Control	13	3.7/4.2 (1.3–6.4)	61.5	0.0

CAP-RAST = Capsulated hydrophilic carrier polymer-radioallergosorbent test.

Table 2. Comparison of clinical data between rhinovirus- and RS virus-induced acute asthma

	Severity score	Admission period days	Wheeze period days	Systemic corticosteroid use, days
Rhinovirus-induced acute asthma	2.0 ± 0.4*	9.0 ± 4.5	6.5 ± 4.1	4.7 ± 2.4
RS virus-induced acute asthma	1.8 ± 0.5	7.7 ± 2.3	4.8 ± 1.8	4.3 ± 2.9

* Mean ± SD.

content in serum was measured with a fluoroenzyme immunoassay kit (Pharmacia, Uppsala, Sweden). Serum cytokines/chemokines were determined using a multi-cytokine detection system (Bio-Rad, Hercules, Calif., USA) following the manufacturer's instructions, measured using a Luminex System (Austin, Tex., USA), and then quantified using Bio-Plex software (Bio-Rad) [15].

Statistical Analysis

Patient characteristic data were evaluated using Pearson's χ^2 test and Fisher's exact test for categorical variables. Multivariate analyses were conducted using multivariate linear regression or multivariate logistic regression analysis, allowing simultaneous assessment of each factor from patients in the acute wheezing group or controls. Age, sex, and atopic status were potential confounders and adjustments were made for the multivariate analyses. Paired data or unpaired data were analyzed using the Wilcoxon or Mann-Whitney U test, respectively. Correlation coefficients for the parameters were calculated using Spearman's rank correlation coefficient analysis. $p < 0.05$ (2-sided) was considered statistically significant. All analyses were performed using a statistical software package (SPSS for Windows, version 18.0; SPSS Japan, Inc., Tokyo, Japan).

Results

Patient Characteristics and Clinical Data

We detected 21 rhinoviruses, 12 RS viruses, 8 enteroviruses including 7 enterovirus type 68 and 1 coxsackievirus, and 7 other viruses including 3 rhinovirus plus RS virus, 3 RS virus plus coxsackievirus, and RS virus plus parainfluenza-3 virus; no viruses were detected in 10 samples, and 4 were not examined in the investigation in a total of 62 patients with acute exacerbations of wheezing. We next compared several clinical data such as the symptom severity score, admission and wheeze period, and systemic corticosteroid use in the 2 major virus groups, i.e. rhinovirus and RS virus. Patient characteristics are shown in table 1. No significant differences for age, sex, or atopic status between each group were found. Twenty-eight patients with acute exacerbation of asthma were treated with intravenous prednisolone for 1 mg/kg/day (total mean dose; 5.3 ± 1.8 mg/kg, mean ± SD, total median dose; 5.5 mg/kg, range 2–9 mg/kg). The admission or wheeze period in patients with rhinovirus-induced acute exacerbation of asthma seemed to be longer than in patients with RS-induced acute exacerbation of asthma although there was no significant difference between the 2 groups (table 2).

Serum Eosinophil Cationic Protein and Cytokines/Chemokines

The serum levels of ECP, IL-5, and IL-6 were significantly elevated in patients with rhinovirus-induced acute exacerbation of asthma compared with controls (fig. 1). In contrast, serum IL-1β and IFN-γ were significantly decreased in patients with rhinovirus-induced acute ex-

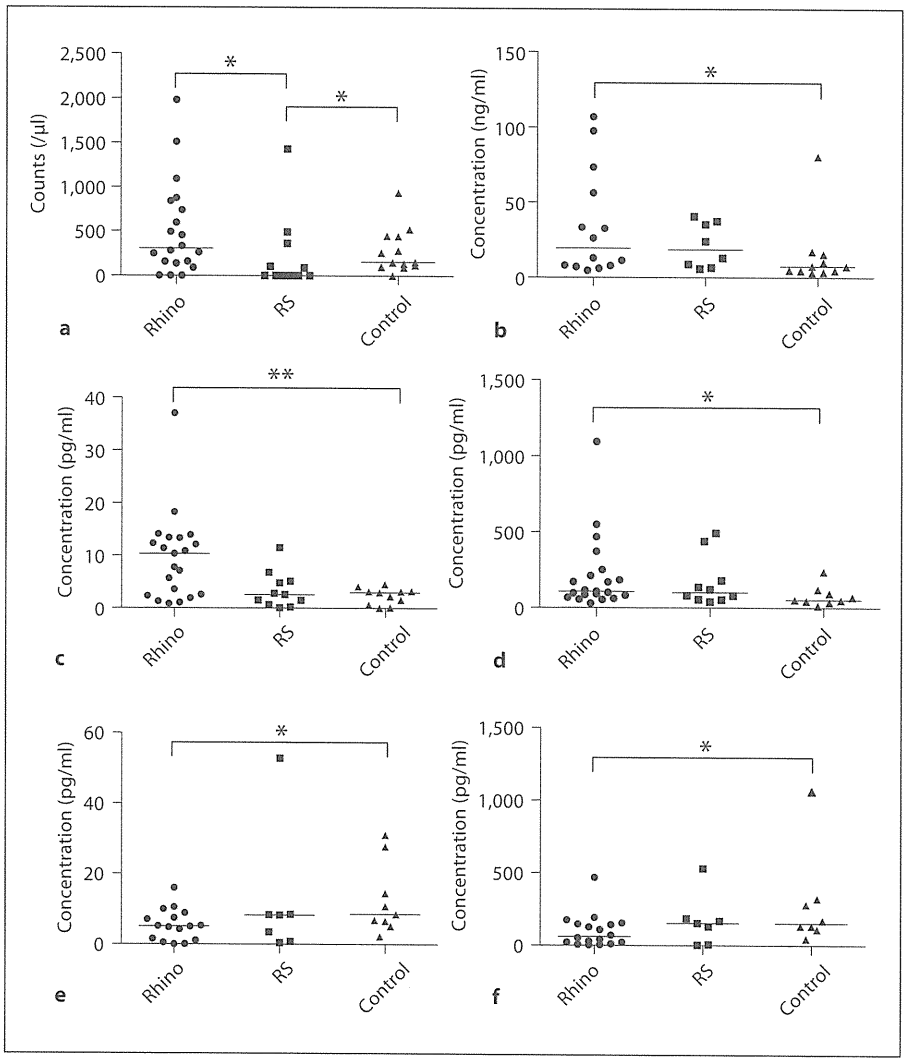

Fig. 1. Comparison of peripheral blood eosinophil counts, serum levels of ECP, and cytokines between rhinovirus- or RS virus-induced acute exacerbation of asthma and controls. **a** Eosinophils. **b** ECP. **c** IL-5. **d** IL-6. **e** IL-1β. **f** IFN-γ. Values are shown for each subject. The median is represented by the horizontal bars. Data were analyzed using the Mann-Whitney U test. * $p < 0.05$; ** $p < 0.01$.

acerbation of asthma compared with controls. On the other hand, in patients with RS virus-induced acute exacerbation of asthma, only the peripheral eosinophil count was significantly decreased compared with that of patients with rhinovirus-induced acute exacerbation of asthma and controls. Other cytokines/chemokines including IL-2, 4, 7, 8, 10, 12, 13, and 17 and TNF-α, GM-CSF, MCP-1, and MIP-1β were not significantly changed in patients with rhinovirus- or RS virus-induced acute exacerbation of asthma or in controls.

Next, we investigated the effects of systemic corticosteroids on these parameters. In virus-induced acute exacerbation of asthma, serum IL-5, IL-6, and G-CSF were significantly reduced after the treatment that included systemic corticosteroids (n = 28) while serum IL-8 was significantly decreased after the treatment that did not included systemic corticosteroids (n = 5) (data not shown). We further examined the effects of systemic corticosteroids on each parameter in the group with rhinovirus- or RS virus-induced acute exacerbation of asthma. The treatments that included systemic corticosteroids significantly reduced the elevated serum ECP, IL-5, and IL-6 levels in rhinovirus-induced acute exacerbation of asthma (fig. 2). Conversely, lowered serum levels of IL-1β and IFN-γ were recovered after the treatments that included systemic corticosteroids (fig. 2). Furthermore, in RS virus-induced acute exacerbation of asthma, the same treatment significantly decreased serum G-CSF although this was not significantly elevated compared with that in controls (fig. 2).

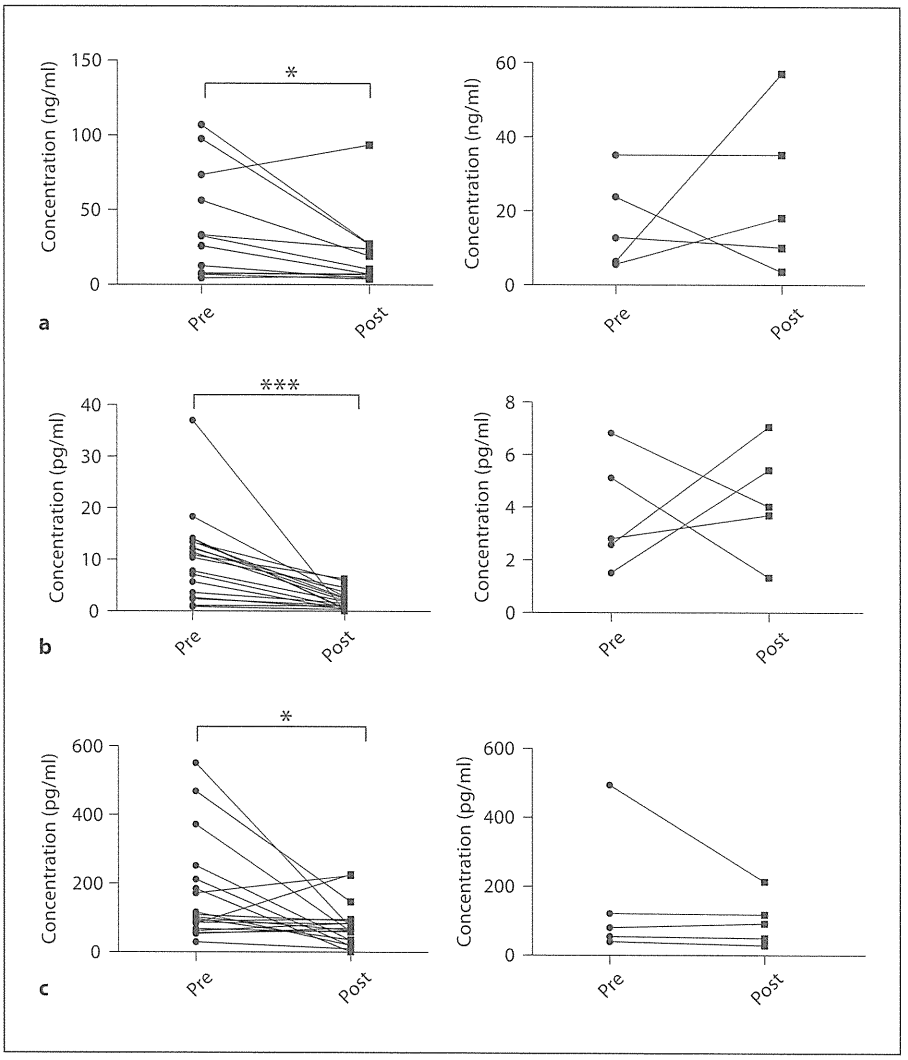

Fig. 2. Effects of treatments that included systemic corticosteroids on serum levels of ECP and cytokines in rhinovirus- (left side in figure) or RS virus- (right side in figure) induced acute exacerbation of asthma. **a** ECP. **b** IL-5. **c** IL-6. Values are shown for each subject. Data were analyzed using the Wilcoxon test. * $p < 0.05$; ** $p < 0.01$; *** $p < 0.001$, pretreatment vs. posttreatment.

Discussion

In this study, we found that the serum levels of ECP, IL-5, and IL-6 in rhinovirus-induced acute exacerbation of childhood asthma were significantly reduced after treatments that included systemic corticosteroids, while those of G-CSF in RS virus-induced acute exacerbation of asthma were significantly reduced after the same treatments. These results suggest that the pathogeneses of rhinovirus- and RS virus-induced acute exacerbation of childhood asthma might be different and that eosinophil activation is involved in rhinovirus-induced acute exacerbation of childhood asthma.

However, at the present time, we do not know the exact mechanism by which rhinoviruses might induce acute exacerbation of asthma and enhance eosinophil activation. A recent report found that, with the sensitive indirect in situ RT-PCR method, rhinoviruses were detected in the mucosal biopsies of 73% of patients with asthma and 22% of nonasthmatic control subjects. Subjects positive for rhinovirus had lower pulmonary function, higher numbers of blood eosinophils and leukocytes, and eosinophilic infiltration in bronchial mucosa [16]. Further evidence suggests a role of deficient IFN-γ [17], IFN-β [18], and type III IFN-λ [19] production in rhinovirus-induced asthma exacerbation and indicates novel mechanisms for the increased susceptibility of subjects with asthma to rhinovirus infection [19, 20]. Our results of lower serum IFN-γ production in rhinovirus-induced acute exacerbation of asthma also confirm these observations. In our study, serum IL-1β was also decreased in patients with rhinovirus-induced acute exacerbation of

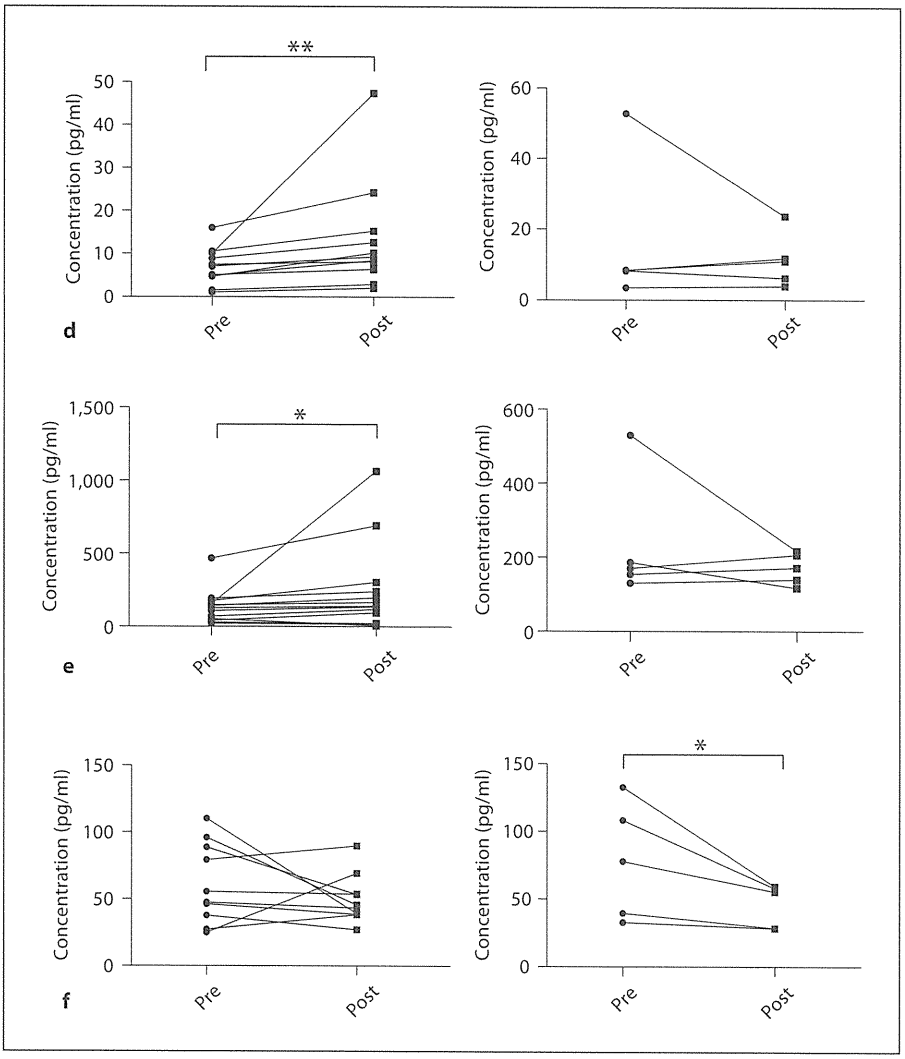

Fig. 2. Effects of treatments that included systemic corticosteroids on serum levels of ECP and cytokines in rhinovirus- (left side in figure) or RS virus- (right side in figure) induced acute exacerbation of asthma. **d** IL-1β. **e** IFN-γ. **f** G-CSF. Values are shown for each subject. Data were analyzed using the Wilcoxon test. * $p < 0.05$; ** $p < 0.01$; *** $p < 0.001$, pretreatment vs. posttreatment.

asthma compared with controls. IL-1β is known to be released from human alveolar macrophages [21], monocytes [22], and tracheal epithelial cells [23]. Although we did not find a report of serum IL-1β in patients with rhinovirus-induced acute exacerbation of asthma, an in vitro study showed that rhinovirus infection induced IL-1β production in supernatants of human tracheal epithelial cells [23]. On the other hand, another report found that IL-1β-derived human monocytes were not detected in experimental rhinovirus infection [22]. We do not know the exact mechanism by which serum IL-1β is decreased in rhinovirus-induced acute exacerbation of asthma. However, various factors including multiple cytokine networks and different sources of IL-β may affect our results for the serum samples in contrast to the in vitro studies.

There are a number of papers relating to experimental rhinovirus infection and the induction of a variety of cellular responses. Human rhinoviruses induce an increase in airway reactivity and epithelial [24] or sputum [25] eosinophils in asthmatic patients. Rhinovirus infection upregulates the expression of intracellular adhesion molecule-1 (ICAM-1) mRNA, the major rhinovirus receptor, and the increased production of IL-1α, IL-1β, IL-6, IL-8, TNF-α, and GM-CSF in supernatants of human tracheal epithelial cells [21]. Similarly, rhinovirus infection upregulates GM-CSF [26], eotaxin, and eotaxin-2 expression in bronchial epithelial BEAS-2B cells [27]. In human airway submucosal glands, eosinophil chemotaxis was augmented during rhinovirus infection [28]. A very recent paper found that rhinovirus infection enhances airway epithelial remodeling through VEGF production [29]. Collec-

tively, evidence suggests that rhinoviruses could induce eosinophil activation, particularly through eosinophil-active cytokines/chemokines such as IL-5, GM-CSF, and eotaxin, as well as an increase in the number of eosinophils.

At present, there is no specific treatment for virus-induced acute exacerbation of asthma. Corticosteroid therapy is one of the most effective treatments for asthma. However, treatment with inhaled corticosteroids does not improve airway inflammation induced by rhinovirus infection [30]. On the other hand, oral glucocorticoids improve lung function and decrease the elevation of serum IL-6, soluble ICAM-1, and ECP [31]. Recently, we reported that treatment that included systemic corticosteroids could decrease serum levels of ECP, IL-5, IL-6, IL-1ra, and IP-10 in acute exacerbation of childhood asthma [32]. In this study, we further found that treatment with systemic corticosteroids decreased serum ECP and IL-5 in rhinovirus-induced acute exacerbation of asthma but not in RS virus-induced acute exacerbation of asthma. In experimental data, Wark et al. [33] reported that rhinovirus infection induced IP-10 and RANTES in the greatest quantities, followed by IL-6 and IL-8, and that dexamethasone partially suppressed IP-10 and TNF-α but was more effective at suppressing RANTES, IL-6, and IL-8 production. Another paper showed that dexamethasone inhibits rhinovirus infection by reducing the surface expression of ICAM-1 and the production of IL-1β, IL-6, and IL-8 in cultured human tracheal epithelial cells [21]. In addition to these reports, our results indicate that systemic corticosteroids might decrease eosinophil activation through IL-5 in rhinovirus-induced acute exacerbation of asthma. Finally, we do not know the mechanism by which serum IL-1β and IFN-γ are increased after treatment that includes systemic corticosteroids in rhinovirus-induced acute exacerbation of asthma. In addition to the in vivo study, the time lag (mean 36 h) between the final day of steroid treatment (mean 5.3 days after admission) and the time samples are taken for post-treatment (mean 6.8 days after admission) may affect the recovery of their values.

Further work is needed to better explore the mechanisms behind the association between asthma exacerbations and rhinovirus or RS virus infections. These studies might ultimately lead to specific treatment to prevent and/or treat the significant burden of acute exacerbation of asthma caused by different virus infections.

Acknowledgements

This study was supported, in part, by Grants-in-Aid for Scientific Research (C) (No. 18591208 and 20591267) from the Ministry of Education, Culture, Sports, Sciences and Technology, the Ministry of Environment Government, and by Gunma Prefecture (Japan). We thank Mrs. Hiroyuki Tsukagoshi and Masakazu Yoshizumi as well as Ms. Mika Saitoh for their excellent technical assistance, and Dr. Makoto Todokoro and other doctors who work for Gunma Children's Medical Center for collecting the samples.

Disclosure Statement

The authors declare that no financial or other conflict of interest exists in relation to the contents of this article.

References

1 Lemanske RF: Viral infections and asthma inception. J Allergy Clin Immunol 2004;114:1023–1026.

2 Black CP: Systematic review of the biology and medical management of respiratory syncytial virus infection. Respir Care 2003;48:209–233.

3 Stein RT, Sherrill D, Morgan WJ, Holberg CJ, Halonen M, Taussig LM, Wright AL, Martinez FD: Respiratory syncytial virus in early life and risk of wheeze and allergy by age 13 years. Lancet 1999;354:541–545.

4 Sigurs N, Bjarnason R, Sigurbergsson F, Kjellman B: Respiratory syncytial virus bronchiolitis in infancy is an important risk factor for asthma and allergy at age 7. Am J Respir Crit Care Med 2000;161:1501–1507.

5 Kneyber MCJ, Steyerberg EW, de Groot R, Moll HA: Long-term effects of respiratory syncytial virus (RSV) bronchiolitis in infants and young children: a quantitative review. Acta Paediatr 2000;89:654–660.

6 Kotaniemi-Syrjänen A, Reijonen TM, Korhonen K, Korppi M: Wheezing requiring hospitalization in early childhood: predictive factors for asthma in a six-year follow-up. Pediatr Allergy Immunol 2002;13:418–425.

7 Singleton RJ, Redding GJ, Lewis TC, Martinez P, Bulkow L, Morray B, Peters H, Gove J, Jones C, Stamey D, Talkington DF, DeMain J, Bernert JT, Butler JC: Sequelae of severe respiratory syncytial virus infection in infancy and early childhood among Alaska Native children. Pediatrics 2003;112:285–290.

8 Sigurs N, Gustafsson PM, Bjarnason R, Lundberg F, Schmidt S, Sigurbergsson F, Kjellman B: Severe respiratory syncytial virus bronchiolitis in infancy and asthma and allergy at age 13. Am J Respir Crit Care Med 2005;171:137–141.

9 Nicholson KG, Kent J, Ireland DC: Respiratory viruses and exacerbations of asthma in adults. BMJ 1993;307:982–986.

10 Johnston SL, Pattemore PK, Sanderson G, Smith S, Lampe F, Josephs L, Symington P, O'Toole S, Myint SH, Tyrrell DA: Community study of role of viral infections in exacerbations of asthma in 9–11 year old children. BMJ 1995;310:1225–1229.

11 Kotaniemi-Syrjänen A, Vainionpää R, Reijonen TM, Waris M, Korhonen K, Korppi M: Rhinovirus-induced wheezing in infancy – the first sign of childhood asthma? J Allergy Clin Immunol 2003;111:66–71.
12 Lemanske RF Jr, Jackson DJ, Gangnon RE, Evans MD, Li Z, Shult PA, Kirk CJ, Reisdorf E, Roberg KA, Anderson EL, Carlson-Dakes KT, Adler KJ, Gilbertson-White S, Pappas TE, Dasilva DF, Tisler CJ, Gern JE: Rhinovirus illnesses during infancy predict subsequent childhood wheezing. J Allergy Clin Immunol 2005;116:571–577.
13 Jackson DJ, Gangnon RE, Evans MD, Roberg KA, Anderson EL, Pappas TE, Printz MC, Lee WM, Shult PA, Reisdorf E, Carlson-Dakes KT, Salazar LP, DaSilva DF, Tisler CJ, Gern JE, Lemanske RF Jr: Wheezing rhinovirus illnesses in early life predict asthma development in high-risk children. Am J Respir Crit Care Med 2008;178:667–672.
14 Nishimuta T, Nishima S, Morikawa A (eds): Japanese Pediatric Society: Japanese Pediatric Guideline for the Treatment and Management of Asthma 2008 (in Japanese). Tokyo, Kyowakikaku, 2008, pp 14–16.
15 Kato M, Tsukagoshi H, Yoshizumi M, Saitoh M, Kozawa K, Yamada Y, Maruyama K, Hayashi Y, Kimura H: Different cytokine profile and eosinophil activation are involved in rhinovirus- and RS virus-induced acute exacerbation of childhood wheezing. Pediatr Allergy Immunol 2010;22:e87–e94.
16 Wos M, Sanak M, Soja J, Olechnowicz H, Busse WW, Szczeklik A: The presence of rhinovirus in lower airways of patients with bronchial asthma. Am J Respir Crit Care Med 2008;177:1082–1089.
17 Brooks GD, Buchta KA, Swenson CA, Gern JE, Busse WW: Rhinovirus-induced interferon-γ and airway responsiveness in asthma. Am J Respir Crit Care Med 2003;168:1091–1094.
18 Wark PA, Johnston SL, Bucchieri F, Powell R, Puddicombe S, Laza-Stanca V, Holgate ST, Davies DE: Asthmatic bronchial epithelial cells have a deficient innate immune response to infection with rhinovirus. J Exp Med 2005;201:937–947.
19 Contoli M, Message SD, Laza-Stanca V, Edwards MR, Wark PA, Bartlett NW, Kebadze T, Mallia P, Stanciu LA, Parker HL, Slater L, Lewis-Antes A, Kon OM, Holgate ST, Davies DE, Kotenko SV, Papi A, Johnston SL: Role of deficient type III interferon-λ production in asthma exacerbations. Nat Med 2006;12:1023–1026.
20 Johnston SL: Innate immunity in the pathogenesis of virus-induced asthma exacerbations. Proc Am Thorac Soc 2007;4:267–270.
21 Tang C, Rolland JM, Ward C, Li X, Bish R, Thien F, Walters EH: Modulatory effects of alveolar macrophages on CD4+ T-cell IL-5 responses correlate with IL-1beta, IL-6, and IL-12 production. Eur Respir J 1999;14:106–112.
22 Stöckl J, Vetr H, Majdic O, Zlabinger G, Kuechler E, Knapp W: Human major group rhinoviruses downmodulate the accessory function of monocytes by inducing IL-10. J Clin Invest 1999;104:957–965.
23 Suzuki T, Yamaya M, Sekizawa K, Yamada N, Nakayama K, Ishizuka S, Kamanaka M, Morimoto T, Numazaki Y, Sasaki H: Effects of dexamethasone on rhinovirus infection in cultured human tracheal epithelial cells. Am J Physiol Lung Cell Mol Physiol 2000;278:L560–L571.
24 Fraenkel DJ, Bardin PG, Sanderson G, Lampe F, Johnston SL, Holgate ST: Lower airways inflammation during rhinovirus colds in normal and in asthmatic subjects. Am J Respir Crit Care Med 1995;151:879–886.
25 de Kluijver J, Evertse CE, Sont JK, Schrumpf JA, van Zeijl-van der Ham CJ, Dick CR, Rabe KF, Hiemstra PS, Sterk PJ: Are rhinovirus-induced airway responses in asthma aggravated by chronic allergen exposure? Am J Respir Crit Care Med 2003;168:1174–1180.
26 Sanders SP, Kim J, Connolly KR, Porter JD, Siekierski ES, Proud D: Nitric oxide inhibits rhinovirus-induced granulocyte macrophage colony-stimulating factor production in bronchial epithelial cells. Am J Respir Cell Mol Biol 2001;24:317–325.
27 Papadopoulos NG, Papi A, Meyer J, Stanciu LA, Salvi S, Holgate ST, Johnston SL: Rhinovirus infection up-regulates eotaxin and eotaxin-2 expression in bronchial epithelial cells. Clin Exp Allergy 2001;31:1060–1066.
28 Furukawa E, Ohrui T, Yamaya M, Suzuki T, Nakasato H, Sasaki T, Kanda A, Yasuda H, Nishimura H, Sasaki H: Human airway submucosal glands augment eosinophil chemotaxis during rhinovirus infection. Clin Exp Allergy 2004;34:704–711.
29 Leigh R, Oyelusi W, Wiehler S, Koetzler R, Zaheer RS, Newton R, Proud D: Human rhinovirus infection enhances airway epithelial cell production of growth factors involved in airway remodeling. J Allergy Clin Immunol 2008;121:1238–1245.
30 Grünberg K, Sharon RF, Sont JK, In 't Veen JC, Van Schadewijk WA, De Klerk EP, Dick CR, Van Krieken JH, Sterk PJ: Rhinovirus-induced airway inflammation in asthma: effect of treatment with inhaled corticosteroids before and during experimental infection. Am J Respir Crit Care Med 2001;164:1816–1822.
31 Yasuda H, Suzuki T, Zayasu K, Ishizuka S, Kubo H, Sasaki T, Nishimura H, Sekizawa K, Yamaya M: Inflammatory and bronchospastic factors in asthma exacerbations caused by upper respiratory tract infections. Tohoku J Exp Med 2005;207:109–118.
32 Kato M, Yamada Y, Maruyama K, Hayashi Y: Serum eosinophil cationic protein and 27 cytokines/chemokines in acute exacerbation of childhood asthma. Int Arch Allergy Immunol 2010;152(suppl 1):62–66.
33 Wark PA, Bucchieri F, Johnston SL, Gibson PG, Hamilton L, Mimica J, Zummo G, Holgate ST, Attia J, Thakkinstian A, Davies DE: IFN-γ-induced protein 10 is a novel biomarker of rhinovirus-induced asthma exacerbations. J Allergy Clin Immunol 2007;120:586–593.

Cancer Science
The official journal of the Japanese Cancer Association

Aberrations of *NEGR1* on 1p31 and *MYEOV* on 11q13 in neuroblastoma

Junko Takita,[1,2,6] Yuyan Chen,[2] Jun Okubo,[2] Masashi Sanada,[3] Masatoki Adachi,[2] Kentaro Ohki,[2] Riki Nishimura,[2] Ryoji Hanada,[4] Takashi Igarashi,[2] Yasuhide Hayashi[5] and Seishi Ogawa[3]

Departments of [1]Cell Therapy and Transplantation Medicine, [2]Pediatrics, and [3]Cancer Genomics Project, Graduate School of Medicine, University of Tokyo, Tokyo; [4]Division of Hematology/Oncology, Saitama Children's Medical Center, Saitama; [5]Gunma Children's Medical Center, Maebashi, Japan

(Received February 9, 2011/Revised May 12, 2011/Accepted May 25, 2011/Accepted manuscript online May 30, 2011/Article first published online July 4, 2011)

MYEOV **and** ***NEGR1*** **are novel candidate gene targets in neuroblastoma that were identified by chromosomal gain in 11q13 and loss in 1p31, respectively, through single nucleotide polymorphism array analysis. In the present study, to assess the involvement of** ***MYEOV*** **and** ***NEGR1*** **in the pathogenesis of neuroblastoma, we analyzed their mutation status and/or expression profiles in a panel of 55 neuroblastoma samples, including 25 cell lines, followed by additional functional studies. No tumor-specific mutations of** ***MYEOV*** **or** ***NEGR1*** **were identified in our case series. Expression of** ***MYEOV*** **was upregulated in 11 of 25 cell lines (44%) and in seven of 20 fresh tumors (35%). The siRNA-mediated knockdown of** ***MYEOV*** **in NB-19 cells, which exhibit high expression of** ***MYEOV,*** **resulted in a significant decrease in cell proliferation (*P* = 0.0027). Conversely, expression studies of** ***NEGR1*** **revealed significantly lower expression of this gene in neuroblastomas at an advanced stage of the disease. Exogenous** ***NEGR1*** **expression in neuroblastoma cells induced significant inhibition of cell growth (*P* = 0.019). The results of these studies provide supporting evidence for** ***MYEOV*** **and** ***NEGR1*** **as gene targets of 11q13 gains and 1p31 deletions in a neuroblastoma subset. In addition, the findings suggest a possible prognostic value for** ***NEGR1*** **in neuroblastoma. (*Cancer Sci* 2011; 102: 1645–1650)**

Neuroblastoma is one of the most common forms of solid tumors in childhood and accounts for approximately 15% of all pediatric cancer deaths.[1] Despite recent advances in chemoradiotherapy, the prognosis for advanced neuroblastoma remains poor, with an approximate 40% 5-year survival, underscoring the importance of developing novel therapeutic modalities on the basis of an understanding of the pathogenesis of neuroblastoma.[1] Conversely, knowledge of the molecular pathogenesis of neuroblastoma is largely limited in terms of targets, except for the role of *MYCN* amplifications in advanced neuroblastoma.[2] Thus, the recent discovery of *ALK* mutations/amplifications in 6–8% of neuroblastomas[3–6] represents a major development in neuroblastoma research because it not only unravels a novel molecular mechanism involved in neuroblastoma development, but could also a basis for the development of molecular-targeted therapies using ALK inhibitors.[3–6] Similar to a number of novel genetic targets discovered recently in other human cancers, *ALK* mutations were identified thorough genome-wide analyses of copy numbers using high-throughput technologies, including high-density single nucleotide polymorphism (SNP) genotyping microarrays.[3–6] A number of recurrent copy number changes other than those of the *ALK* locus have been identified by genome-wide copy number analysis of neuroblastoma, including losses of 1p31, 3q13, 9p24, 15q11, and 16p13, and high-grade amplifications of 1p36, 7q21, 7q31, 11q13, and 15q13,[3] which may provide important clues for the identification of novel target genes. In fact, several candidate target genes of these common deletions and amplifications have been identified, including *MYEOV* as the target of gains/amplifications in 11q13[7] and *NEGR1* as a candidate tumor suppressor in 1p31 deletions.[8] Previously, *MYEOV* was reported as a putative transforming gene within the 11q13 amplicons in multiple myeloma,[9] whereas *NEGR1* was described as a member of the IgLON (limbic system-associated membrane protein [LAMP]/opioid-binding cell adhesion molecule [OBCAM]/neurotrimin subgroup of the immunoglobulin superfamily) family of cell adhesion molecules.[8] However, the involvement of these genes aberrations in the pathogenesis of neuroblastoma remains unknown. Therefore, in the present study we focused on the abnormalities in both genes and assessed their role, both genetically and functionally, in the pathogenesis of neuroblastoma.

Materials and Methods

Specimens. Primary neuroblastoma specimens were obtained at the time of surgery or biopsy from patients who had been diagnosed with neuroblastoma and had been admitted to Tokyo University Hospital, Saitama Children's Medical Center, or various other hospitals between November 1993 and October 2006. Patients were staged according to the International Neuroblastoma Staging System,[10] with five patients classified as Stage 3 and 25 classified as Stage 4. The clinicopathological findings for all patients are listed in Table 1. Twenty-five neuroblastoma cell lines were also used in the present study (Table 2). The SCMC-N2 series was established in our laboratory;[11] the SJNB series and UTP-N-1[12] were generous gifts from Drs A.T. Look (Department of Pediatric Oncology, Dana Farber Cancer Institute, Harvard Medical School, Boston, USA) and A. Inoue (Department of Molecular Biology, Toho University School of Medicine, Tokyo, Japan), respectively; all other cell lines were obtained from the Japanese Cancer Resource Cell Bank (http://cellbank.nibio.go.jp/wwwjcrbj.htm, accessed 7 Sep 2008). All cells were maintained in RPMI 1640 medium (Gibco-BRL, Grand Island, NY, USA) supplemented with 10% fetal bovine serum in a humidified atmosphere containing 5% CO_2 at 37°C.

Semi-quantitative RT-PCR. Total RNA was extracted from the 25 cell lines and 20 frozen stocked tumors using Isogen reagent (Nippon Gene, Osaka, Japan) according to the manufacturer's instructions and was subjected to reverse-transcription reactions to synthesize cDNA using the SuperScript Preamplification System for First Strand cDNA synthesis (Life Technologies, Rockville, MD, USA). Semi-quantitative RT-PCR analysis for *MYEOV*, *CCND1*, and *NEGR1* gene expression was performed as described previously[13] using the primer sets listed in Table S1, available as an accessory publication to this paper. The concentration of the cDNA was normalized against that of *β-actin*, used as an internal control. The signal intensity of *MYEOV* and *CCND1* expression was estimated using NIH

[6]To whom correspondence should be addressed.
E-mail: jtakita-tky@umin.ac.jp

doi: 10.1111/j.1349-7006.2011.01995.x

Table 1. Clinical data for the neuroblastoma cases in the present study

Case no.	Age	Stage	Diagnosis	Histology	*MYCN* amplification	Outcome
1	4 years 2 months	4	C	NBL poorly dif.	+	Alive
2	2 years 4 months	4	C	NBL poorly dif.	+	Alive
3	4 years	4	C	NBL poorly dif.	+	Alive
4	3 years	4	C	NBL poorly dif.	–	Alive
5	1 year 5 months	4	C	NBL poorly dif.	–	Alive
6	10 day	3	C	NBL dif.	–	Alive
7	4 years	4	C	NBL poorly dif.	–	Dead
8	4 years 2 months	4	C	NBL poorly dif.	–	Alive
9	2 years	3	C	GNB well dif.	–	Alive
10	10 years	4	C	NBL	–	Dead
11	4 years	4	C	NBL	+	Dead
12	3 years	3	C	NBL	+	Alive
13	11 years 9 months	4	C	NBL poorly dif.	–	Alive
14	6 months	3	MS	GNB	–	Alive
15	7 months	4	MS	NBL poorly dif.	–	Dead
16	4 years	4	C	NBL	+	Dead
17	4 years 9 months	4	C	NBL	–	Dead
18	7 months	4	MS	NBL	–	Alive
19	2 years	4	C	NBL poorly dif.	+	Alive
20	3 years	4	C	NBL	+	Dead
21	8 years	4	C	NBL poorly dif.	–	Alive
22	2 years 3 months	4	C	NBL	+	Alive
23	4 years	4	C	NBL	+	Dead
24	5 months	4	C	NBL	–	Alive
25	5 years	4	C	NBL	–	Dead
26	4 years 10 months	4	C	NBL	–	Alive
27	7 years	4	C	NBL poorly dif.	+	Dead
28	1 year 6 months	3	C	NBL	–	Alive
29	1 year 8 months	4	C	NBL	–	Alive
30	8 months	4	C	NBL	–	Alive

C, clinical; MS, mass screening program; NBL, neuroblastoma; NBL poorly dif., poorly differentiated neuroblastoma; GNB, ganglioneuroblastoma; GNB well dif., well-differentiated ganglioneuroblastoma.

Table 2. Neuroblastoma cell lines used in the present study

Cell line	MYCN amplification
CHP-134	–
GOTO	+
IMR-32	+
LAN-1	+
LAN-2	+
LAN-5	+
NB-1	–
NB-16	+
NB-19	+
NB-69	–
NH-12	+
SCMC-N2	+
SCMC-N4	+
SCMC-N5	+
SJNB-1	–
SJNB-2	+
SJNB-3	–
SJNB-4	+
SJNB-5	+
SJNB-6	+
SJNB-7	+
SJNB-8	+
SK-N-SH	–
TGW	+
UTP-N-1	+

Image 1.61 software (Wayne Rasband; National Institutes of Health, Bethesda, MD, USA).

Quantitative RT-PCR. To quantify the expression levels of *NEGR1*, real-time PCR (RQ-PCR) analysis was performed using the QuantiTect SYBR Green PCR kit (Qiagen, Tokyo, Japan) with an iCycler iQ real-time PCR detection system (Bio-Rad Japan, Tokyo, Japan). The primer sets used for the RQ-PCR are listed in Table S1 and the PCR conditions were as described previously.[13] For the purpose of normalization, relative expression levels were calculated by dividing the expression level of the respective gene by that of *β-actin*.

Mutational analysis of *MYEOV* and *NEGR1* genes. Genetic screening for *MYEOV* and *NERG1* genes in 25 cell lines was performed by denaturing HPLC (DHPLC) using the WAVE System Model 4500 (Transgenomic, Omaha, NE, USA), as described previously.[14] The primer sets used in the present study are listed in Table S1.

Bisulfate modification and methylation-specific PCR. Bisulfate modification of genomic DNA was performed as described previously.[15] For methylation-specific PCR (MSP), approximately 10 ng bisulfite-treated DNA was amplified with primers for both the methylated and unmethylated sequences. Reaction products were separated by electorophoresis on a 2.0% agarose gel. The primer sets for methylation-specific PCR analysis are listed in Table S1.

Knockdown of *MYEOV* using siRNA. The functional roles of the *MYEOV* gene in neuroblastoma cells was assessed using gene knockdown with siRNA.[16] The siRNA was designed and synthesized for silencing *MYEOV* (Invitrogen, Carlsbad, CA,

doi: 10.1111/j.1349-7006.2011.01995.x

USA). The siRNA duplex had the following sequences: 1132 sense, 5′-UCA ACG CCC ACU CUA AAG GCU UCU C-3′; and 1132 antisense, 5′-GAG AAG CCU UUA GAG UGG GCG UUG A-3′. A chemically synthesized non-silencing siRNA duplex that had no known homology to any mammalian gene was used as a control for non-specific silencing events and had the following sequences: sense, 5′-UUC UCC GAA CGU GUC ACG UdT dT-3′; and antisense, 5′-ACG UGA CAC GUU CGG AGA AdT dT-3′. Gene knockdown was achieved in NB-19, CHP-134 and PF-SK-1 cells using HiPerFect transfection reagent (Qiagen, Valencia, CA, USA) according to the manufacturer's instructions.

Transient transfection. The expression vector (pME18S) containing the full-length *EcoRI-Xba1* fragment of the *NEGR1* cDNA was transfected into NB-19, SJNB-7, and PF-SK-1 cells using the lipofection method according to the manufacturer's instructions (Qiagen).[11] Briefly, 1.5×10^5 cells were seeded in a six-well plate and incubated in 1.6 mL RPMI 1640 (Gibco-BRL) with 10 μL Effectance reagent (Qiagen), 3.2 μL Enhancer (1:8) (Qiagen), 10 μL Effectene (Qiagen), and 0.4 μg expression vector. Cells were counted 72 h after transfection.

Statistical analysis. Expression of the *NEGR1* gene was compared between favorable and unfavorable cases of neuroblastomas using the Mann–Whitney *U*-test. Exact 95% confidence intervals (CI) of the proportions were calculated on the basis of binomial distribution. The Kruskal–Wallis test was used to compare the functional effects of *MYEOV* inhibition and *NEGR1* expression in neuroblastoma cells.

Results

Gain and high-grade amplification of 11q13 involving the *MYEOV* locus in neuroblastoma. In the present series, gains of chromosome 11q13 were detected in multiple neuroblastoma cases.[3] Within this gain, a high-grade amplification was found in a single case with Stage 4 disease (Case 22; Fig. 1a). The critical amplicon that had minimum overlapping amplification/gain was found in a 340-kb region exclusively containing *MYEOV*, located 360 kb upstream from the *CCND1* locus[7] (Fig. 1a). Previously, *MYEOV* had been identified as a putative transforming gene based on the NIH/3T3 tumorigenicity assay[9] and was shown to be highly expressed in a subset of multiple myelomas harboring t(11;14)(q13;q32).[7] We further examined the expression patterns of *MYEOV* in a total of 45 neuroblastoma samples using semi-quantitative RT-PCR analysis, in which 11 of 25 cell lines (44%) and seven of 20 fresh tumors (35%) showed higher expression levels of *MYEOV* compared with the median expression level (*MYEOV/β-actin* signal intensity = 1.4; Fig. 1b). Although most tumors exhibited increased expression of both *CCND1* and *MYEOV*, Case 22 showed high expression of *MYEOV* but not *CCND1* (Fig. 1c). Mutational analysis of the coding region of *MYEOV* was also performed in 25 cell lines, but no tumor-specific mutations were detected.

Homozygous deletion on 1p31 detected in neuroblastoma. Detection of homozygous deletions was also of interest because they provide an important clue in pinpointing tumor suppressor loci. In an allele-specific copy number analyzer for GeneChip (CNAG) and allele-specific copy number analysis using anonymous references (AsCNAR), homozygous deletions could be identified as the loss of both parental alleles, even in the presence of significant components of normal tissues.[3] In the present study, 70 homozygous deletions were identified at 50 independent loci in the neuroblastoma samples. Unfortunately, we were not able to completely exclude the possibility that some may represent copy number variations (CNV) rather than real homozygous deletions, because paired DNA was available only in four primary neuroblastoma cases and many homozygous deletions were found in established neuroblastoma cell

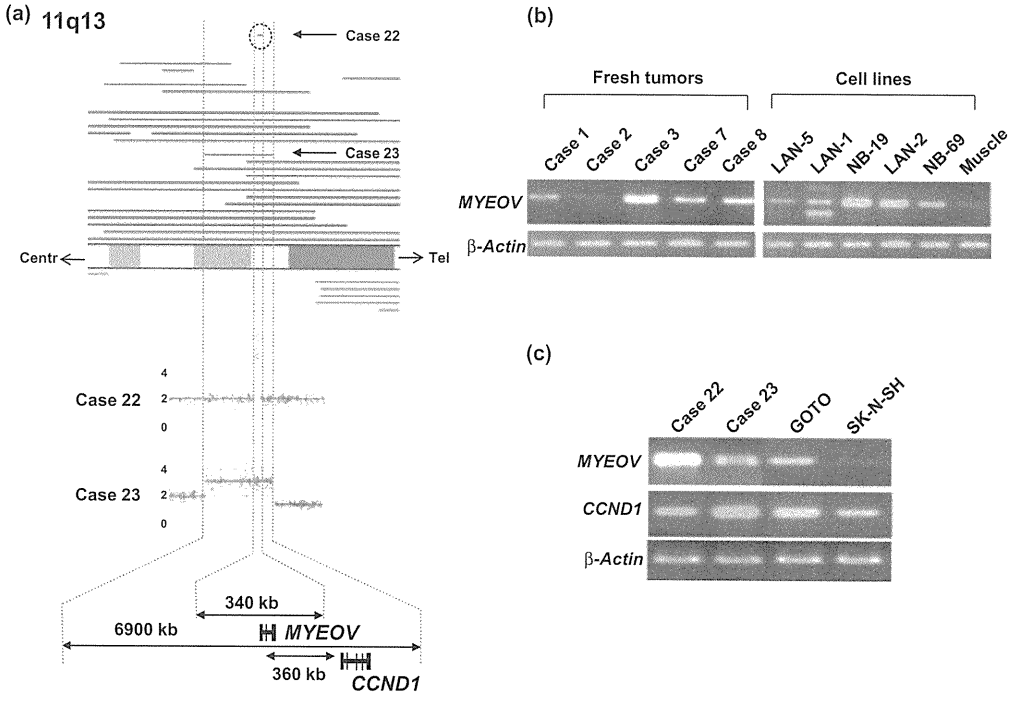

Fig. 1. Gains and high-grade amplification on chromosome 11q13 in neuroblastoma. (a) A common 340-kb region having copy number (CN) gains contains a single known gene, *MYEOV*. In addition, *CCND1* is frequently contained in CN gains at 11q13, but mapped outside the minimum region of common CN gains. Red bars, gains ($3 < CN < 5$); green bars, losses ($CN = 1$); light red bar (circled), high-grade amplification ($CN \geq 5$). (b) Representative results of *MYEOV* expression in fresh tumors and cell lines (RNA from normal muscle was used as a control). (c) Expression of *MYEOV* and *CCND1* in Cases 22 and 23 (RNA from normal muscle was used as a control). The expression of *MYEOV* in Case 22 tended to be higher than that in Case 23. tel, telomere; centr, centromere.

lines. Complete loss of genetic material at eight loci was confirmed by genomic PCR (data not shown).

Of the 70 homozygous deletions identified, we focused on a homozygous deletion involving a 370-kb region at 1p31 in NB-19. This region contains a part of *NEGR* (exon 1 and a part of intron 1), a unique candidate target gene, which was also disrupted by a translocation in another cell line, namely SJNB-6 (Fig. 2a,b). Because *NEGR1* encodes a member of the IgLON family of cell adhesion molecule sand has been reported to be a putative tumor suppressor gene in ovarian cancer,[8] we examined its expression in neuroblastoma cases in the present study to evaluate the clinical impact of *NEGR1* expression. As shown in Figure 2(c), *NEGR1* expression was absent or very low in 10 of 25 (40%) cell lines, as determined by semi-quantitative RT-PCR (Fig. 2c). In quantitative RT-PCR analysis using fresh tumor samples (20 fresh advanced-stage tumors and an additional 20 cases of early stage tumors), the expression of the *NEGR1* gene was significantly lower in advanced-stage tumors compared with early stage tumors ($P = 0.0041$; Fig. 2c). Similarly, the expression of the *NEGR1* gene was significantly lower in patients who died compared with patients who survived ($P = 0.018$; Fig. S1). Mutation analysis was also performed in neuroblastoma cell lines, but no tumor-specific mutations were detected. Methylation analysis of the promoter region of *NEGR1* using 10 neuroblastoma cell lines without *NEGR1* expression did not reveal any tumor-specific methylation pattern in neuroblastoma cell lines or fresh neuroblastoma samples (data not shown).

Functional analyses of *MYEOV* and *NEGR1* in neuroblastoma cell lines. We further evaluated the oncogenic potential of *MYEOV* using siRNA-mediated gene knockdown in the NB-19 cell line, which highly expresses *MYEOV*. As shown in Figure 3(a,b). When *MYEOV* expression was suppressed by siRNA, NB-19 cells exhibited retarded growth compared with the growth of control cells ($P = 0.0027$), indicating that MYEOV positively regulates cell proliferation (Fig. 3a,b). Similar results were obtained in CHP-134 and PF-SK-1 cells (Fig. S2). To assess the tumor suppressor function of *NEGR1* in neuroblastoma cells, we generated an *NEGR1* expression vector that was transiently transfected into NB-19 cells, in which *NEGR1* is homozygously deleted. Expression of *NEGR1* significantly suppressed the proliferation of NB-19 cells compared with mock transfection ($P = 0.019$; Fig. 3c,d). In addition, the *NEGR1* expression vector was transiently transfected into SJNB-7 and PF-SK-1 cells, in which *NEGR1* expression is absent. Following transfection into these cell lines, profound inhibition of cell proliferation was observed for both SJNB-7 and PF-SK-1 cells expressing *NEGR1* (Fig. S3).

Discussion

In the present study, we showed that *MYEOV* and *NEGR1* are candidate gene targets of 11q13 gain and 1p31 deletion, respectively, in a neuroblastoma subset. To our knowledge, this is the first report to describe aberrations of *MYEOV* and *NEGR1* in neuroblastoma.

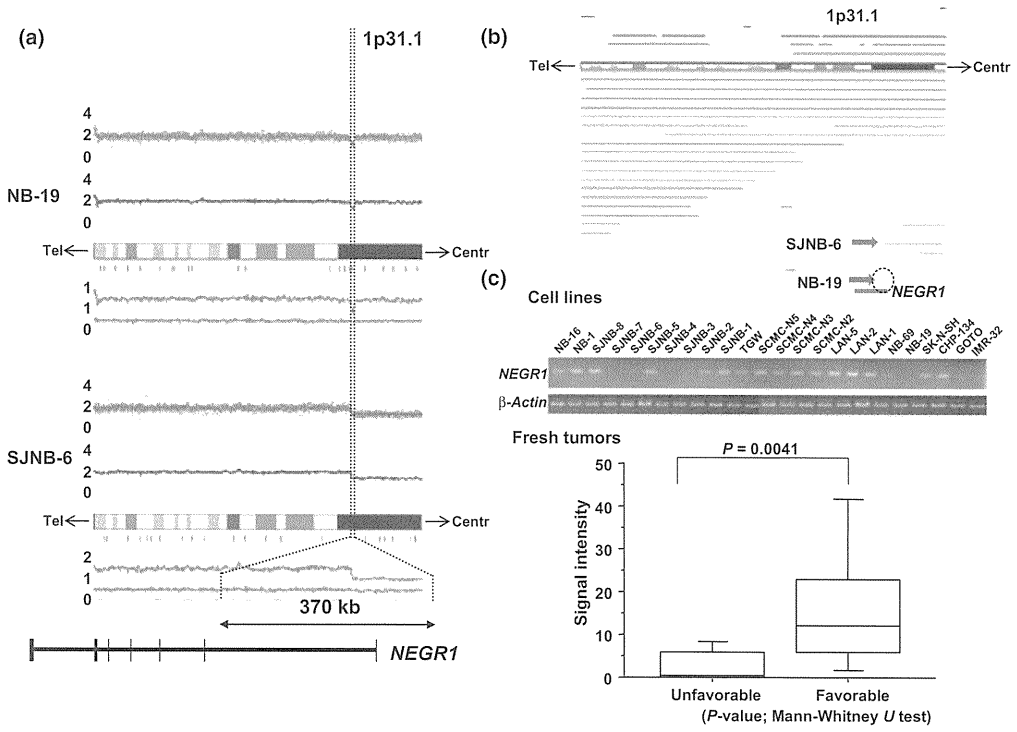

Fig. 2. *NEGR1* as a candidate tumor suppressor gene in neuroblastoma. (a) Deletion mapping of 1p31.1 disclosed a homozygous deletion spanning a 370-kb region in the NB-19 cell line, which contains part of *NEGR1* as the only structural gene. The *NEGR1* gene is also disrupted in intron 1 by the breakpoint of a segmental duplication at 1p31.1 in another neuroblastoma cell line (SJNB-6). For each panel, total copy numbers (tCN; red dots), moving averages of tCN for five consecutive single nucleotide polymorphisms (SNP; blue line), an ideogram of the relevant chromosome, the location of heterozygous SNP calls (green bars), and allele-specific copy numbers (AsCN) averaged for five consecutive SNP (red and green lines for larger and smaller alleles, respectively) are plotted. Note that the CN are expressed in terms of "observed" signal ratios between tumor and reference samples, where the baseline is adjusted to 2 for tCN plots and to 1 for AsCN. (b) Summary of CN abnormalities of 1p31.1 in neuroblastoma. Red bars, gains ($3 < CN < 5$); green bars, losses ($CN = 1$); light green bar (circled), homozygous deletion ($CN = 0$). A homozygous deletion detected in NB-19 and a chromosomal rearrangement detected in SJNB-6 are indicated by the red arrows. The location of *NEGR1* is shown by the blue line. (c) *NEGR1* expression in neuroblastoma. Top panel: representative result of *NEGR1* expression in neuroblastoma cell lines showing frequently reduced expression levels in a subset of neuroblastoma cell lines. Bottom graph: expression of the *NEGR1* gene as measured by quantitative PCR was significantly lower in tumors with an unfavorable outcome than in tumors with a favorable outcome ($P = 0.0041$, Mann–Whitney *U*-test). tel, telomere; centr, centromere.

doi: 10.1111/j.1349-7006.2011.01995.x

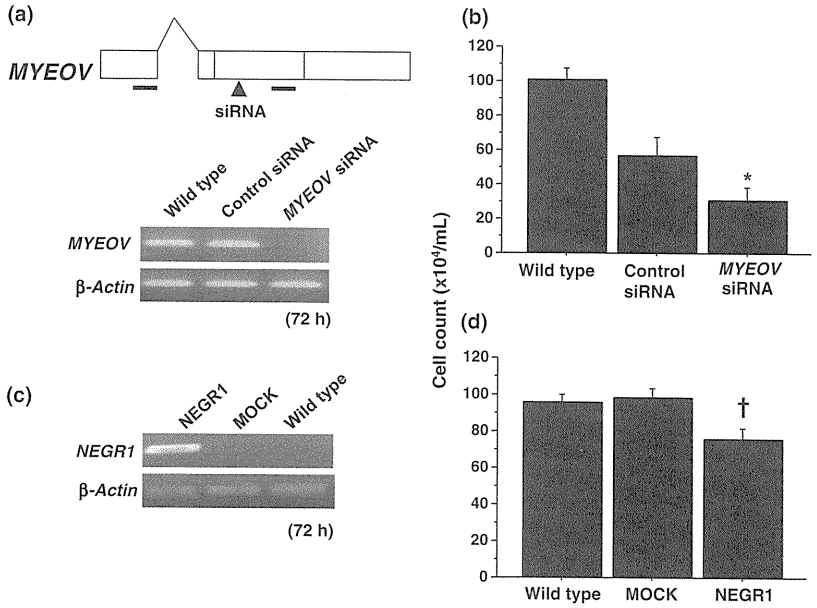

Fig. 3. Effect of *MYEOV* inhibition by siRNA on cell growth and effect of *NEGR1* on cell growth in neuroblastoma cells. (a) Confirmation of siRNA-mediated gene knockdown using semi-quantitative RT-PCR analysis. Following siRNA treatment, *MYEOV* mRNA was absent in treated cells; however, abundant *MYEOV* expression was detected in wild-type and control cells. (b) Effect of *MYEOV* inhibition by siRNA transfected into NB-19 cells on cell growth. Cell growth was impaired cell growth in siRNA-transfected cells compared with that of control cells (*P = 0.0027, Kruskal–Wallis test). (c) Analysis (RT-PCR) of NB-19 cells transfected with the pME18S vector. Mock-transfected and wild-type cells were used as controls. (d) The growth of cells transiently expressing *NEGR1* was impaired compared with that of mock-transfected and wild-type cells (†P = 0.019, Kruskal–Wallis test).

Initially, *MYEOV* was reported as a gene that was possibly co-overexpressed with *CCND1* in some cases of multiple myeloma with t(11;14)(q13;q32); later, it was shown to be co-amplified and co-overexpressed with *CCND1* in a subset of esophageal squamous cell carcinomas, breast cancers, gastric cancers, and colorectal cancers.[7,17–19] Although the major genetic targets of these rearrangements and amplifications have been shown to be *CCND1*, in some breast cancer cases the 11q13 amplicon exclusively contained *MYEOV* and not *CCDN1*, suggesting a *CCDN1*-independent oncogenic role for *MYEOV*.[7] The oncogenic role of *MYEOV* has also been investigated in functional studies, showing that *in vitro* siRNA-mediated knockdown of *MYEOV* resulted in inhibition of proliferation, invasion, and migration of colorectal cancer cell lines.[19] In our neuroblastoma cases, *MYEOV* was overexpressed in approximately 30% of primary neuroblastoma cases, with seven cases showing gain/amplification of MYEOV. We also confirmed that *MYEOV* was the only gene found in the common gain/amplicon at 11q13 and that proliferation of neuroblastoma cell lines was inhibited by siRNA-mediated *MYEOV* knockdown, supporting an oncogenic role for *MYEOV* in some neuroblastoma cases. Although several studies have revealed that *MYEOV* amplification is associated with poor prognosis in multiple myeloma, esophageal squamous cell carcinoma, and breast cancer,[7,18,20] the clinical impact of *MYEOV* gain/amplification or overexpression in neuroblastoma is unclear and requires further evaluation.

The *NEGR1* gene is a single gene found in one of the recurrent deletions at 1p31. Although the *NEGR1* locus is known as one of the most common CNV regions,[21] we also identified a neuroblastoma cell line in which *NEGR1* was disrupted in by gene rearrangement, supporting the fact that *NEGR1* is one of the target genes in neuroblastoma. In ovarian cancer, *NEGR1* is a putative tumor suppressor gene encoding one of the IgLON cell adhesion family members, namely OPCML, and it plays a central role in the establishment and remodeling of the central nervous system.[22] Notably, OPCML has been shown to exhibit functional characteristics of a tumor suppressor gene in epithelial ovarian cancer.[23] In our analysis, expression of *NEGR1* was substantially reduced in 43% of advanced-stage tumors without 1p31 deletions/rearrangement. In addition, re-expression of *NEGR1* in the NB-19 cell line with homozygous deletion of *NEGR1*, as well as in other neuroblastoma cell lines that did not express *NEGR1*, resulted in the inhibition of cell growth, suggesting that *NEGR1* is a candidate tumor suppressor gene in neuroblastoma and may have possible prognostic value. Although expression of OPCML in ovarian cancers is suppressed or reduced mainly through epigenetic mechanisms,[23] tumor-specific methylation was not detected in neuroblastoma cells in the present study. The mechanisms for the absence of *NEGR1* in the tumors without homozygous deletion, mutation, and methylation were not clear in the present study. We cannot role out the possibility that mutations are harbored in the promoter region of *NEGR1* with consequent gene inactivation. Furthermore, *NEGR1* was often heterozygously deleted, but not mutated or methylated, in neuroblastoma; most deletions occur in tumors at advanced stages, suggesting that *NEGR1* has haploinsufficient effects on advanced disease in neuroblastoma.

In conclusion, the results of the present study suggest that *MYEOV* at 11q13 and *NEGR1* at 1p31 are functional gene targets in a subset of neuroblastoma. Further studies on both genes will expand these pathways and provide insights into the progression of neuroblastoma, as well as possibly enabling the development of novel therapeutics based on targeting MYEOV and NEGR1 in neuroblastoma.

Acknowledgments

The authors thank Mrs Matsumura M, Mrs Hoshino N, Mrs Yin Y and Mrs Saito F for their excellent technical assistance. The authors also express their appreciation to Drs A.T. Look (Harvard Medical University, Boston, MA, USA) and Dr. A. Inoue (St. Jude Children's Research Hospital, Memphis, TN, USA), for their generous gifts of neuroblastoma cell lines. This work was supported by Research on Measures for Intractable Diseases, Health, and Labor Sciences Research Grants; the

Ministry of Health, Labor and Welfare via a grant for Research on Health Sciences focusing on Drug Innovation; by the Japan Health Sciences Foundation; and by the Core Research for Evolutional Science and Technology, Japan Science and Technology Agency.

Disclosure Statement

The authors have no conflicts of interest.

References

1 Brodeur GM. Neuroblastoma: biological insights into a clinical enigma. *Nat Rev Cancer* 2003; **3**: 203–16.
2 Brodeur GM, Seeger RC, Schwab M, Varmus HE, Bishop JM. Amplification of N-myc in untreated human neuroblastomas correlates with advanced disease stage. *Science* 1984; **224**: 1121–4.
3 Chen Y, Takita J, Choi YL *et al.* Oncogenic mutations of ALK kinase in neuroblastoma. *Nature* 2008; **455**: 971–4.
4 Mosse YP, Laudenslager M, Longo L *et al.* Identification of ALK as a major familial neuroblastoma predisposition gene. *Nature* 2008; **455**: 930–5.
5 Janoueix-Lerosey I, Lequin D, Brugieres L *et al.* Somatic and germline activating mutations of the ALK kinase receptor in neuroblastoma. *Nature* 2008; **455**: 967–70.
6 George RE, Sanda T, Hanna M *et al.* Activating mutations in ALK provide a therapeutic target in neuroblastoma. *Nature* 2008; **455**: 975–8.
7 Janssen JW, Cuny M, Orsetti B *et al.* MYEOV: a candidate gene for DNA amplification events occurring centromeric to CCND1 in breast cancer. *Int J Cancer* 2001; **102**: 608–14.
8 Ntougkos E, Rush R, Scott D *et al.* The IgLON family in epithelial ovarian cancer: expression profiles and clinicopathologic correlates. *Clin Cancer Res* 2005; **11**: 5764–8.
9 Brecht M, Steenvoorden AC, Luf S, Bartram CR, Janssen JW. Rearrangement and expression of myeov and hst in NIH/3T3 transfectants: a caveat for the interpretation of DNA transfection analyses. *Oncol Rep* 2007; **17**: 1127–31.
10 Smith EI, Haase GM, Seeger RC, Brodeur GM. A surgical perspective on the current staging in neuroblastoma: the International Neuroblastoma Staging System proposal. *J Pediatr Surg* 1989; **24**: 386–90.
11 Takita J, Hayashi Y, Nakajima T *et al.* The p16 (CDKN2A) gene is involved in the growth of neuroblastoma cells and its expression is associated with prognosis of neuroblastoma patients. *Oncogene* 1998; **17**: 3137–43.
12 Inoue HK, Shirao T. Neurite formation induced in neuroblastoma cells and genetically altered non-neuronal cells. *J Electron Microsc* 1997; **46**: 497–502.
13 Takita J, Ishii M, Tsutsumi S *et al.* Gene expression profiling and identification of novel prognostic marker genes in neuroblastoma. *Genes Chromosom Cancer* 2004; **40**: 120–32.
14 Donohoe TJ, Sintim HO, Sisangia L *et al.* Utility of the ammonia-free Birch reduction of electron-deficient pyrroles: total synthesis of the 20s proteasome inhibitor, clasto-lactacystin beta-lactone. *Chemistry* 2005; **11**: 4227–38.
15 Takita J, Yang HW, Chen YY *et al.* Allelic imbalance on chromosome 2q and alterations of the caspase 8 gene in neuroblastoma. *Oncogene* 2001; **20**: 4424–32.
16 Moss AC, Lawlor G, Murray D *et al.* ETV4 and Myeov knockdown impairs colon cancer cell line proliferation and invasion. *Biochem Biophys Res Commun* 2006; **345**: 216–21.
17 Janssen JW, Vaandrager JW, Heuser T *et al.* Concurrent activation of a novel putative transforming gene, myeov, and cyclin D1 in a subset of multiple myeloma cell lines with t(11;14)(q13;q32). *Blood* 2000; **95**: 2691–8.
18 Carneiro A, Isinger A, Karlsson A *et al.* Prognostic impact of array-based genomic profiles in esophageal squamous cell cancer. *BMC Cancer* 2008; **8**: 98.
19 Lawlor G, Doran PP, MacMathuna P, Murray DW. MYEOV (myeloma overexpressed gene) drives colon cancer cell migration and is regulated by PGE_2. *J Exp Clin Cancer Res* 2010; **29**: 81.
20 Moreaux J, Hose D, Bonnefond A *et al.* MYEOV is a prognostic factor in multiple myeloma. *Exp Hematol* 2010; **38**: 1189–98.
21 Jarick I, Vogel CI, Scherag S *et al.* Novel common copy number variation for early onset extreme obesity on chromosome 11q11 identified by a genome-wide analysis. *Hum Mol Genet* 2011; **20**: 840–52.
22 Funatsu N, Miyata S, Kumanogoh H *et al.* Characterization of a novel rat brain glycosylphosphatidylinositol-anchored protein (Kilon), a member of the IgLON cell adhesion molecule family. *J Biol Chem* 1999; **274**: 8224–30.
23 Sellar GC, Watt KP, Rabiasz GJ *et al.* OPCML at 11q25 is epigenetically inactivated and has tumor-suppressor function in epithelial ovarian cancer. *Nat Genet* 2003; **34**: 337–43.

Supporting Information

Additional Supporting Information may be found in the online version of this article:

Fig. S1. *NEGR1* expression in 30 neuroblastoma cases.

Fig. S2. Effect of siRNA inhibition of *MYEOV* on cell growth in CHP-134 and PF-SK-1 cells.

Fig. S3. Effect of *NEGR1* on cell growth in the neuroblastoma cell lines PF-SK-1 and SJNB-7.

Table S1. Primer sequences used in the present study.

Please note: Wiley-Blackwell are not responsible for the content or functionality of any supporting materials supplied by the authors. Any queries (other than missing material) should be directed to the corresponding author for the article.

doi: 10.1111/j.1349-7006.2011.01995.x

J Gastroenterol (2011) 46:639–647
DOI 10.1007/s00535-010-0330-5

ORIGINAL ARTICLE—LIVER, PANCREAS, AND BILIARY TRACT

Development of an experimental model of cholestasis induced by hypoxic/ischemic damage to the bile duct and liver tissues in infantile rats

Fumiaki Toki · Atsushi Takahashi · Makoto Suzuki · Sayaka Ootake · Junko Hirato · Hiroyuki Kuwano

Received: 21 December 2009 / Accepted: 10 August 2010 / Published online: 25 February 2011

Abstract
Background We aimed to develop experimental models of hypoxia/ischemia-induced cholestasis using neonatal and infantile rats.
Methods Hypoxia/ischemia was induced in the bile duct (BD) by injecting prostaglandin (PG) at birth and/or by coagulation of the hepatic artery (CHA) at about 3 weeks after birth. The rats were divided into 6 groups: control; PG-injected; sham-operated with or without PG; CHA; and CHA + PG. CHA was also performed in adult rats. Liver specimens and blood samples were obtained at 5 weeks after birth, and immunohistochemical and biochemical examinations were performed.
Results (1) BD proliferation with fibrosis (BDPF) was found in the intrahepatic portal tract in the CHA and CHA + PG groups. Low-grade BDPF was observed in the PG group. (2) Cyst formation in the extrahepatic BD (EBD) was observed in the porta hepatis of some rats in the CHA and CHA + PG groups. In these groups, the number of peribiliary vascular plexuses (PVPs) decreased. BD proliferation and infiltration of inflammatory cells were observed in the EBD wall in the CHA + PG group. (3) Ki-67 was expressed in BD and EBD cells in the CHA + PG group. (4) BDPF was not detected in adult rats with CHA. (5) Serum liver function tests indicated obstructive changes in the EBD in the CHA and CHA + PG groups.
Conclusion Reduced blood flow in the EBD during infancy induced BDPF and obstructive changes in the EBD, which may, along with immature PVP and inflammatory changes in the EBD, contribute to hypoxia/ischemia of the EBD.

Keywords Bile duct proliferation with fibrosis · Cholestasis · Hypoxia/ischemia · Inflammation · Neonate · Infant

F. Toki (✉) · A. Takahashi · M. Suzuki · S. Ootake · H. Kuwano
Pediatric Surgical Unit, Department of General Surgical Science, Gunma University Hospital, 3-39-15 Showa-machi, Maebashi, Gunma 371-8511, Japan
e-mail: ftoki@gcmc.pref.gunma.jp

J. Hirato
Department of Pathology, Gunma University Hospital, Maebashi, Japan

Introduction

Cholestasis is sometimes diagnosed in neonates and infants [1–3], generally in association with neonatal hepatitis [3], congenital biliary atresia [4–6], and other disorders [1–3]. In addition, cholestasis also occurs occasionally in cases of total parenteral nutrition [7–9], bacterial or hypovolemic shock [9–11], treatment with some drugs [12], perinatal asphyxia [13], and after liver transplantation [14, 15]. Bile duct (BD) hypoxia/ischemia is thought to be a possible cause of cholestatic disorders [1, 3, 4, 6, 9, 13–15]. The BD epithelium—particularly the extrahepatic BD (EBD) and at least the major intrahepatic BDs—depends on the blood supply from the hepatic artery, and the BD epithelium is susceptible to injury when the arterial blood flow is compromised [14–16].

An experimental model of cholestasis has been developed in adult animals by the ligation of the hepatic artery and peribiliary vascular plexus (PVP), which supply the blood flow to the BD epithelium [17]. Pickett and Briggs [18] have demonstrated that BD obstruction develops after ligation of the hepatic artery in fetal sheep. In addition, the

administration of prostaglandin (PG) E, a vasodilator, leads to the development of a persistent ductus venosus and ductus arteriosus in neonatal animals [19–21]. Theoretically, the persistence of the ductus arteriosus induces a decrease in the blood flow in the hepatic artery [22]. Therefore, it is hypothesized that cholestasis in neonatal small animals would be induced by hypoxia/ischemia in the BDs and/or liver tissue, which could be achieved by PG treatment and/or ligation of the hepatic artery.

To clarify whether the induction of hypoxia/ischemia in the BDs, EBD, and/or liver tissue of neonatal and infantile rats induces cholestasis in the liver, we injected PG in neonatal rats soon after birth and performed coagulation of the hepatic artery (CHA) in early infantile rats. Histological examinations, including immunohistochemical staining for Ki-67, and biochemical serum liver function tests were performed to evaluate the injury of the BDs, EBD, and liver tissue. In addition, because it has been reported that only CHA did not induce cholestasis in adult rats [17], CHA in adult rats was performed to examine the effects of CHA on the BD and liver tissue of adult rats.

Materials and methods

Animal model and experimental protocol

Just-born Wistar rats were divided into the following 6 groups according to the treatment administered: (1) only saline injection, control (C) group; (2) only PG injection, PG group; (3, 4) sham operation with or without PG injection, SHAM ± PG groups; (5) only CHA, CHA group; and (6) CHA and PG injection, CHA + PG group. PGE_1 (Prostandin20; Ono Pharma, Osaka, Japan) or saline was injected in the newborn rats by following the protocol proposed by Yokozawa [21]. PGE_1 (1 μg/0.1 ml) or the same volume of saline was injected subcutaneously within 12 h of birth and 24 h after the first injection. All neonatal rats injected with PGE_1 survived without the loss of body weight. The operations in the SHAM, CHA, and CHA + PG groups were performed between 18 and 24 days after birth.

The livers and blood samples were obtained at 5 weeks after birth (2 weeks after the operation) and histological and clinical examinations were performed. Immunohistochemical staining for Ki-67 was also performed. In addition, CHA was performed in adult Wistar rats (weighing about 300 g). The liver specimens of adult CHA rats and control rats were taken at 2 weeks after the operation.

All experiments were performed at the animal center of the Gunma University and were in accordance with the guidelines of the Ethics Committee of the Gunma University (Permission number 07-065).

Operative procedures

Midline laparotomy was performed under ether anesthesia. The following procedures were performed under a magnifying lens. Surgery in the rats in the SHAM groups was performed by separating and lifting the hepatic artery from the EBD and portal vein. In the rats in the CHA and CHA + PG groups, CHA was performed after the hepatic artery was separated and lifted from the EBD and the portal vein. The coagulation was performed at the mid-portion of the lifted artery. An outline of the operative procedures is shown in Fig. 1. About 60% of the operated rats survived for up to 1 week after the operation, and these rats were used for further examinations.

Histological examinations

The liver specimens were fixed in formalin and embedded in paraffin. The sections that were cut along the maximum area of the liver specimen, including the porta hepatis, were stained with hematoxylin–eosin and Azan-Mallory. Histological examination of the large intrahepatic portal tract and porta hepatis was performed.

To evaluate the degree of BD proliferation with fibrosis (BDPF), we selected 4 sites of the large intrahepatic portal tract in the Azan-Mallory-stained sections and produced computer-generated images of the sites; the sites were examined according to the following procedures. The extent of BDPF was evaluated by 2 methods. In the first method, 4 grades were established on the basis of the extent of BDPF in the interlobular space between the portal tracts. The grading was as follows: 0, no BDPF; 1, slight BDPF in the interlobular space; 2, BDPF in half of the interlobular space

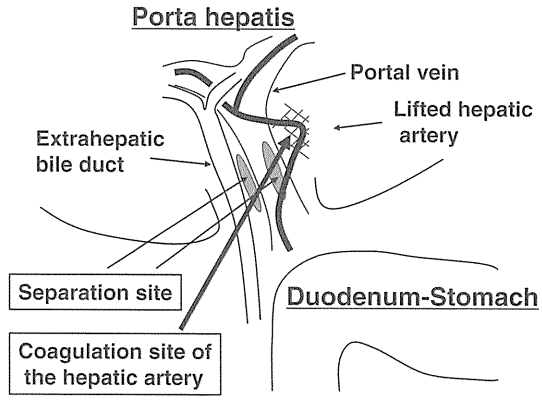

Fig. 1 Schema of the operative procedures. The sham operation was performed by separating and lifting the hepatic artery from the extrahepatic bile duct (EBD) and portal vein, without coagulation of the hepatic artery (CHA). In the CHA and CHA + prostaglandin injection (PG) groups, the hepatic artery was separated and lifted from the EBD and portal vein, and subsequently, the hepatic artery was coagulated. The site of CHA is indicated by *lattice oblique lines*

between the portal tracts; and 3, almost complete BDPF in the interlobular space between the portal tracts. The scoring method was developed on the basis of the method reported by Beaussier et al. [17] with some modification. The computer-generated images were reviewed by 3 examiners. In the second method, evaluation was performed by determining the average number of BDs in the portal tract.

In the porta hepatis, we examined the degree of BD proliferation, PVP distribution in the EBD wall, the presence or absence of EBD lining cells, and inflammatory changes in the EBD wall. Sections in which we did not find the EBD were excluded from further examinations. The degree of BD proliferation was evaluated by the number of BDs, according to the following 4 grades: 0, presence of a few BDs; 1, slight increase in the number of BDs; 2, about a twofold increase in the number of BDs; and 3, more than a twofold increase in the number of BDs. The degree of PVP distribution was evaluated by the number of vessels in each arbitrary unit length around the outer layer of the EBD. The degree of BD cell injury was evaluated by determining the percentage of damaged BD cells/normal BD cells. The presence of inflammation in the EBD wall was judged by the existence of infiltration of inflammatory cells in the inner layer of the EBD wall.

Immunohistochemical staining for Ki-67

Immunohistochemical staining for Ki-67 was performed using a mouse anti Ki-67 monoclonal antibody (MIB-5; DAKO, Glostrup, Denmark) and a streptavidin–biotin staining kit (Nichirei, Tokyo, Japan).

Biochemical examination of blood samples

The serum samples were examined for total bilirubin, alanine transaminase (ALT), γ-glutamyl transpeptidase (γ-GTP), and bile acid.

Statistical analysis

Statistical analysis was performed using a one- or two-tailed Student's *t*-test and the Kruskal–Wallis test; p values of <0.05 were considered significant.

Results

Representative histological findings of the intrahepatic portal tract and porta hepatis in each group and groupwise analysis of the extent of BDPF in the intrahepatic portal tract in each group

Representative images of the intrahepatic portal tracts in all groups are shown in Fig. 2a–f. In the CHA and CHA + PG groups, BDPF was observed in large intrahepatic portal tracts. Part of the BDPF was extended in the peripheral zone of the portal tract. We did not observe histopathological changes in the hepatic parenchyma in any group.

The extent of BDPF in the intrahepatic portal tracts in each group is shown in Fig. 3 and the numbers of BDs in the intrahepatic portal tracts in each group are shown in Fig. 4. The extent of BDPF and the number of BDs in the CHA and CHA + PG groups were significantly higher than those in the C, PG, and SHAM groups. The extent of BDPF in the CHA + PG group was significantly higher than that in the CHA group. The extent of BDPF in the PG group was significantly higher than that in the C group.

Cyst formation was found in the porta hepatis in 2 out of 8 rats in the CHA + PG group and 1 out of 8 rats in the CHA group (Fig. 5a). The cyst wall was mainly composed of BD lining cells (Fig. 5b). No cyst formation was found in the rats in the SHAM group ($n = 10$).

The results of the histological examinations of the porta hepatis are shown in Figs. 6 and 7, and Table 1. BD proliferation was observed in the CHA and CHA + PG groups, but not in the C, PG, and SHAM groups (Fig. 6a–c). The degree of BD proliferation in the CHA and CHA + PG groups was significantly higher than that in the C, PG, and SHAM groups (Table 1).

The number of PVPs in the outer layer of the EBD wall in the C and PG groups was significantly higher than that in the SHAM, CHA, and CHA + PG groups (Fig. 6d–f, Table 1). The number of PVPs in the SHAM groups was significantly higher than that in the CHA and CHA + PG groups (Table 1).

The number of damaged BD lining cells in the CHA and CHA + PG groups was significantly higher than that in the C, PG, and SHAM groups (Table 1).

The infiltration of inflammatory cells in the inner layer of the EBD wall was observed in 3 out of 7 rats in the CHA + PG group (Fig. 7a). These 3 rats exhibited marked extension of BDPF (Fig. 7b).

Results of the immunohistochemical staining for Ki-67

The results of the immunohistochemical staining for Ki-67 are shown in Fig. 8 and Table 2. The immunohistochemical staining revealed that the hepatocytes and BD cells in almost all of the rats in the C, PG, and SHAM groups were negative for Ki-67. Ki-67 was expressed in the hepatocytes and BD cells of rats in the CHA and CHA + PG groups (Fig 8a, b). The rate of positive expression of BD cells in the CHA + PG group was significantly higher than that in the PG and SHAM groups (Table 2).

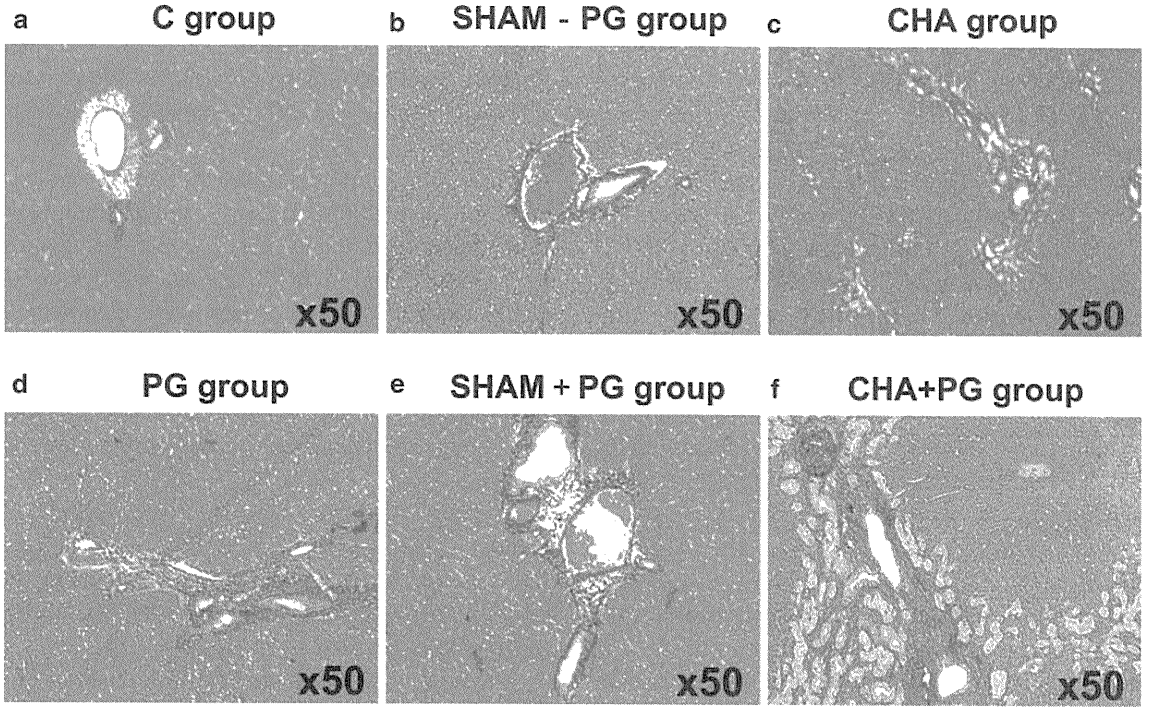

Fig. 2 Representative images of Azan-Mallory staining of the intrahepatic portal tract in the C (**a**), SHAM without PG (**b**), CHA (**c**), PG (**d**), SHAM with PG (**e**), and CHA + PG groups (**f**). The specimens were obtained at 5 weeks after birth. *C* control, *SHAM* sham operation, *PG* prostaglandin injection, *CHA* coagulation of the hepatic artery. **a–f** ×50

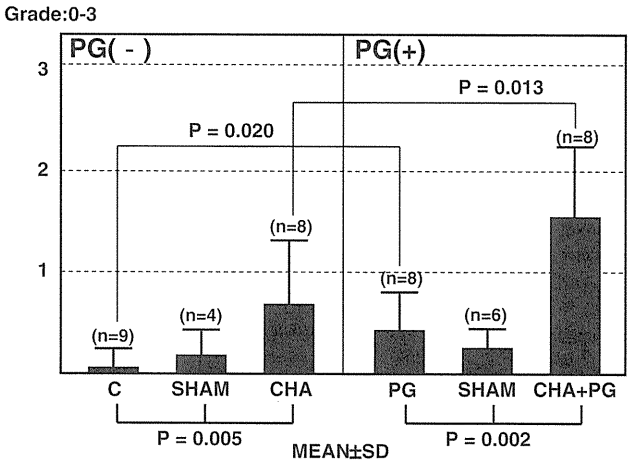

Fig. 3 The extent of bile duct proliferation with fibrosis in the intrahepatic portal tract in each group. *C* control group, *SHAM* sham operation group, *PG* prostaglandin injection group, *CHA* coagulation of the hepatic artery group, *CHA + PG* CHA and PG group

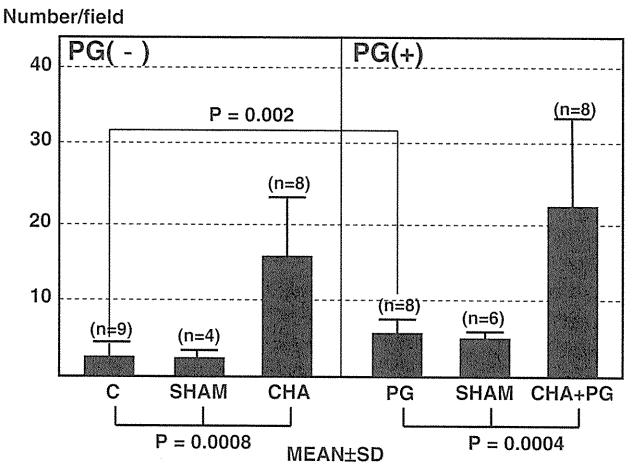

Fig. 4 The number of bile ducts in the intrahepatic portal tract in each group. *C* control group, *SHAM* sham operation group, *PG* prostaglandin injection group, *CHA* coagulation of hepatic artery group, *CHA + PG* CHA and PG group

Results of the examination of adult rats

The results of the histological analysis of adult rats are shown in Table 3. The number of BDs in adult CHA rats was greater than that in the adult control rats, but the number was smaller than those in the infantile rats in the CHA and CHA + PG groups. The extent of BDPF and the number of PVPs were similar in the adult rats in the CHA and C groups.

Results of the serum liver function tests

The results of the serum liver function tests are shown in Table 4. The concentrations of total bilirubin, ALT, γ-GTP, and bile acid in the CHA and CHA + PG groups